EFFECT OF FIBER ADDITION ON THE PERFORMANCE OF PRELOADED CFRP STRENGTHENED CONCRETE BEAMS

by

Kareem Helal Helal

A Thesis Presented to the Faculty of the
American University of Sharjah
College of Engineering
in Partial Fulfillment
of the Requirements
for the Degree of

Master of Science in
Civil Engineering

Sharjah, United Arab Emirates

December, 2017

© 2017 Kareem Helal. All rights reserved.

Acknowledgement

Firstly, I would like to recognize the continuous guidance and support of Dr. Sherif Yehia, my thesis advisor, and Drs. Rami Hawileh and Jamal A. Abdalla, my thesis co-advisors.

I would also wish to thank Engineers Ahmed and Rayyan for their assistance throughout the thesis and Mr. Ansari for his assistance during the testing stages of this thesis.

I would also like to extend special thanks and appreciation to my family for their encouragement and motivation throughout this program.

Last but not least, I would like to thank my company SPME Middle East General Contracting LLC. And my mentors, Jason Dodson, Chris Hill and Dave Clark for their unlimited support and guidance.

Abstract

The aim of this study is to evaluate the effect of fiber addition on the performance of Reinforced Concrete (RC) beams that have been externally strengthened in flexure using Carbon Fiber Reinforced Polymer (CFRP) sheets. Steel, synthetic and hybrid fibers (mix of steel and synthetic fibers) with a volume fraction of 0.5 % were added to the concrete matrix to prepare 15 beams. The experimental program consisted of three groups; 1) control beams without strengthening, 2) beams strengthened without preloading, and 3) beams preloaded to a stress level corresponding to 0.67 of yield stress (fy) of the steel reinforcement before strengthening with CFRP. A steel reinforcement ratio of 0.55% was used for all beams. Eight beams were tested for groups one and two as control (with and without strengthening) and seven beams were pre-loaded before strengthening to simulate the RC beams behavior and conditions at the repair stage. Test results showed that the addition of fibers improved the flexural capacity, crack initiation and propagation, post cracking behavior and ductility of the beams. All beams strengthened after preloading also showed better performance than that of the control beams. Synthetic fiber was found to improve the ductility of the RC beams by 81% when compared to the control specimen without fibers. Additionally, steel fibers caused a strength increase of up to 64% when compared to the control beams. The hybrid mix of fibers provided a combination of benefits from steel and synthetic fiber contributions. Applicability of ACI 440 equations to predict the capacity of fiber reinforce concrete beams was also investigated. The predicted results were in good agreement with the obtained experimental data.

Keywords: Strengthening, CFRP, Fiber Reinforced Concrete, Preloading, Steel Fiber, Synthetic Fiber

Table of Contents

Abstract……..5
List of Figures 8
List of Tables 9
Chapter 1. Introduction 10
1.1. Thesis Objectives 10
1.2. Research Significance 11
1.3. Thesis Organization 12
Chapter 2. Background and Literature Review.....13
2.1. FRP Properties 13
2.2. Literature Review.....14
2.3. ACI-440 17
2.4. Current Practice.....18
Chapter 3. Methodology 19
Chapter 4. Experimental Program.....21
4.1. Important Parameters 21
4.2. Material properties 21
4.2.1. Concrete 21
4.2.2. Reinforcement 22
4.2.2.1. Steel fiber properties – Dramix 3D 23
4.2.2.2. Synthetic fiber properties – STRUX 90/40.....24
4.2.2.3. V-wrap C200H (CFRP sheets) 24
4.3. Test Setup.....27
Chapter 5. Results and Analysis 28
5.1. Results of Experimental Investigation 28
5.2. Load-Deflection Results for Control Beams.....31
5.3. Load-Deflection Results for Strengthened Beams.....32
5.4. Load-Deflection Curves for Preloaded Beam 33
5.5. Cracking Load for First Five Cracks.....34
5.6. Effect of Preloading on CFRP Contribution 35
Chapter 6. Conclusion and Future Work 45
References……46

APPENDIX A - MATERIALS.....49
APPENDIX B – FAILURE MODES 51
APPENDIX C – CONTROL CALCULATIONS.....56
APPENDIX D – CONTROL CALCULATIONS 64
Vita……...74

List of Figures

Figure 1 - Comparison of Ultimate Load for all Test Samples [12] 17
Figure 2 - CFRP Installation Process 18
Figure 3 - Steel Cages with Formwork and Strain Gauges 19
Figure 4 - Preloading Process 20
Figure 5 - Finishing CFRP Installation on all Beams 20
Figure 6 - Compressive Strength Testing 22
Figure 7 - Stress - Strain Curve for Steel Used 23
Figure 8 - Stress-Strain Behavior of CFRP vs. GFRP and Mild Steel [15] 25
Figure 9 - Cross Section Details of Study Beams 26
Figure 10 - Elevation View of Study Beam with Loading 26
Figure 11 - Test Setup and instrumentations 27
Figure 12 - Flexural Failure of Synthetic Fiber Control Beam 29
Figure 13 - Delamination Failure of Strengthened Beam 29
Figure 14 - Delamination Failure of Strengthened Beams 30
Figure 15 - Delamination Failure 30
Figure 16 - Load-Deflection Curves for Control Beams 31
Figure 17- Load-Deflection Curves for Strengthened Beams 32
Figure 18 - Load-Deflection Curves for Preloaded Beams 33
Figure 19 - Comparison between Plain Test Samples 36
Figure 20 - Comparison between Steel Fiber Test Samples 37
Figure 21 - Comparison between Synthetic Fiber Test Samples 38
Figure 22 - Comparison between Hybrid Test Samples 39
Figure 23 - Comparison between Control Test Samples 40
Figure 24 - Comparison between Ultimate Capacities of Beams vs Theoretical 41
Figure 25 - Comparison between Strengthened Test Samples 42
Figure 26 - Comparison between Preloaded Test Samples 43
Figure 27 - Comparison between Strengthened/Preloaded Beams and Theoretical Capacity 43

List of Tables

Table 1 - Properties of Different Strengthening Materials 13
Table 2 - Properties of Reinforcing Steel 22
Table 3 - Actual Properties of Steel Used..... 23
Table 4 - Steel Fiber Properties 23
Table 5 - Synthetic Fiber Properties 24
Table 6 - Fiber Properties (Dry) 24
Table 7 - Cured Laminate Properties..... 25
Table 8 - Summary of Samples for Experimental Program..... 27
Table 9 – Summary of Results from Experimental Investigation 28
Table 10 - Crack Loads for first Five Cracks 34
Table 11 - Comparison between Plain Test Samples 35
Table 12 - Comparison between Steel Fiber Test Samples 37
Table 13 - Comparison between Synthetic Fiber Test Samples 38
Table 14 - Comparison between Hybrid Test Samples 39
Table 15 - Comparison between Control Test Samples 40
Table 16 - Comparison between Strengthened Test Samples..... 41
Table 17 - Comparison between Preloaded Test Samples..... 42
Table 18 - Summary of Loads for First 5 Cracks for Test Beams..... 44

Chapter 1. Introduction

Carbon Fiber Reinforced Polymers (CFRP) are increasingly being used as external strengthening materials to compensate for structural deficiencies in Reinforced Concrete (RC) members. Some causes of these structural deficiencies are building use modification, severe environmental exposure, and imperfections during design and construction stages.

The ongoing efforts to strengthen and rehabilitate existing RC structures are enhanced by the advances in composite material development. These advanced composite materials allow FRP's to be bonded to the exterior surface of different RC members to provide additional flexural, shear and compression capacities [1]. Research efforts have focused on the stress-strain behavior of different types of FRP materials in addition to their overall behavior at yield or failure. Additionally, a study performed by 4-point loading RC beams strengthened with GFRP to failure has concluded that the presence of stresses in the member at the time of repair impacts the ultimate capacity of the RC member [2]. Other studies have concluded that the initial loading that the beam is subjected to affects the efficiency of the FRP strengthening by reducing the stiffness of the RC member [3]. The addition of steel or synthetic fiber transforms concrete into a pseudo-ductile material, thus improving its resistance to crack formation and propagation, impact strength and ductility [4].

Reinforcement ratio, concrete strength, stresses in reinforcement, strengthening materials and repair technique are some of the factors that affect the benefit of the strengthening method. In the current study, stresses in reinforcement and repair technique will be evaluated to determine contribution of CFRP strengthening to the flexural capacity of preloaded fiber RC beams.

1.1. Thesis Objectives

Due to the recent developments in the field of external strengthening, the effect of strengthening on reinforced concrete elements has been investigated over the past few years. However, the literature has limited research on the use of fiber in the concrete matrix coupled with external CFRP strengthening. The main objective of this research

is to evaluate the effect of fiber addition, CFRP strengthening and preloading on the flexural performance of reinforced concrete beams.

1.2. Research Significance

At the end of the service life of a reinforced concrete (RC) structure, the economic feasibility of repairing or demolishing these structures comes into question. However, modern techniques such as Non-Destructive Testing (NDT) or Structural Health Monitoring (SHM) can be utilized to optimize the maintenance process and avoid latter cost and time implications at the end of a service life. Generally, repairing structures can be done with state of the art technology that has been introduced and documented to provide economic alternatives to demolition through extending the life of the existing structure.

CFRP sheets are becoming progressively more valued in the engineering community since it can be used to increase the strength of existing structural elements while having desirable fiber properties in terms of fatigue resistance, ductility, etc. CFRP sheets can be useful in several applications such as:

- Changing function of a reinforced concrete structure.
- Overcoming design or construction flaws.

The aim of this research is to utilize CFRP laminates to augment the flexural capacity of fiber reinforced concrete beams that have been preloaded in order to determine the actual strength contribution of the CFRP laminates in comparison to strengthening done to beams without pre-loading in literature. The different stress levels developed in steel are going to determine the change in concrete micro-structure and also, to the bond between the concrete and reinforcing rebar. Additionally, to control cracking and damage to the concrete microstructure, 3 types of reinforcement techniques are applied to the concrete matrix to enhance its ductility and post stress behaviour. This includes synthetic fibers, steel fibers and a hybrid combination of both. The aim of the fiber addition is to control cracking and enhance the contribution from the CFRP strengthening.

1.3. Thesis Organization

The study is presented through the following chapters –

- Chapter 1: Introduction: provides a discussion of the problem statement and the highlights the relevance of this study. This chapter also presents the objectives of the proposed study for this thesis.
- Chapter 2: Background: highlights the most relevant previous studies and published literature.
- Chapter 3: Methodology: discusses the planned work to achieve the objective of this study.
- Chapter 4: Experimental Program: explains the experimental work that will be done and highlights material properties and other important parameters.
- Chapter 5: Results: presents the results and discusses the effect of different variables on the results obtained.
- Chapter 6: Conclusion: concludes the thesis and provides recommendations for future work.

Chapter 2. Background and Literature Review

Properties of FRP strengthening material, previous research efforts found in the literature, current practice and ACI 440 guide for the design and construction are briefly discussed in this chapter to identify parameters that might affect the proposed investigation. The fiber addition to the concrete matrix greatly improves ductility and reduces the rate of crack formation and propagation.

This chapter discusses previous research efforts in the field of strengthening and the introduction of fibers into concrete. Several efforts have been directed towards the field of strengthening due to the expansion in the construction industry which involves several design changes during project construction, in addition to building function changes.

2.1. FRP Properties

Different types of FRP materials are available for external strengthening. The main differences are strength and durability properties. Table 1 summarizes some of the main differences between these materials [2].

Table 1 - Properties of Different Strengthening Materials

Material	Ultimate Strength (MPa)	Elastic Modulus (GPa)	Failure Strain (%)
Glass FRP	517-1207	30-55	2-4.5
Carbon FRP	1200-2410	147-165	1-1.5
Aramid FRP	1200-2068	50-74	2-2.6
Steel	483-690	200	>10

The most prevalent type of FRP is Carbon FRP due to its relatively higher ultimate strength and availability. Some of the main advantages of CFRP include [2]

- Very high elastic modulus
- High tensile strength to weight ratio
- Very low coefficient of linear thermal expansion

2.2. Literature Review

Strengthening techniques for RC structures have been the focus of numerous researches in order to prolong the service life of structures that are subjected to rapidly varying loading requirements and harsh environmental conditions. This introduces the need for economic and effective retrofitting techniques to increase structural capabilities of different RC members that have been damaged by overloading and deterioration [3]. There are several alternative materials that can be used to strengthen RC structures such as Basalt FRP (BFRP). Carbon FRP (CFRP), Glass FRP (GFRP), Aramid (AFRP) and many more. Additionally, progress in composite material developments has led to different strengthening techniques being used; one of which is the use of fiber reinforced polymers (FRP) that is bonded to the appropriate part of the member to enhance its shear or flexural capacity. The use of FRP has several advantages that include superior mechanical properties and ease of application to different structural members [1]. Using this technique involves attaching FRP sheets or plates to the RC members by means of an epoxy adhesive which enables them to have significant contributions to the overall capacity of the structural members. This approach is suitable for compensating for structural deficiencies resulting from loading conditions or deterioration. Several experimental studies have been carried out to investigate the effect of FRP strengthening on RC beams in shear and flexure [5]. However, some of these studies have indicated that the failure modes of the retrofitted beams can impose limitations on the contribution of the FRP strengthening. Some of the failure modes include FRP delamination and de-bonding of concrete layers which generally occur at loads that are considerably lower than the theoretical capacity of the strengthened beams [1, 6]. Moreover, another promising technique for structural strengthening is the Near Surface Mounding (NSM) where circular CFRP or GFRP materials are installed into slits that are made on the concrete cover of the structural element. It generally requires minimal preparation and much lower installation time compared to CFRP sheets that are externally bonded using epoxy adhesive [7]. CFRPs are vastly used is the concrete strengthening industry due to their relatively high strength to weight ratio. CFRPs are generally characterized by high tensile strength and good chemical and temperature resistance.

A study conducted by Hawileh et al. [9] tested 5 RC beams using four-point bending testing configuration and loaded till failure by means of displacement control loading. Strain gauges were used to obtain strain readings. The study consisted of Five RC beams have sections 120mm x 240mm reinforced with two 10mm diameter bars and closed spaced stirrups to avoid shear failure. The beams were strengthened with 1 Layer of CFRP (BC), 1 Layer of GFRP (BG), and hybrid combinations of both. Table 2 shows the results of the 4-point loading tests done on all beams.

Table 2 - Summary of Results for Test Beams

Specimen	P_u (kN)
B (control)	58.78
BC	92.44
BG	76.84
BGC	107.59
BGCG	116.41

BC= Bottom CFRP, BG= Bottom GFRP, BGC = Bottom GFRP and CFRP, BGCG = Bottom GFRP, CFRP and GFRP

The study concluded that hybrid combinations of CFRP and GFRP sheets are able to increase the load carrying capacity of the strengthened RC beams by up to 98%. In addition to that, increased ductility at failure is very beneficial in terms of providing additional warning signs before failure; this enables precautionary actions to be taken in a timely manner.

Furthermore, research conducted by Attari et al. [10] discusses the efficiency of external strengthening for reinforced concrete beams using FRP to improve strength, ductility and stiffness. The study concluded that GFRP and CFRP can achieve strength increases of up to 114%; however, this increase is accompanied by a slight reduction in ductility [10]. The importance of ductility in RC applications is greatly emphasized but the benefits of doubling the load carrying capacity of the member is a suitable justification for a minor loss in ductility.

Additionally, in an article titled “Strengthening of Preloaded RC Beams Using Hybrid Carbon Sheets,” Zhishen Wu et al. [11] discuss the effect of using hybrid continuous carbon fiber sheets to strengthen RC beams subjected to service loads of 40 or 60% of steel yielding. Table 3 show the beam designations and results of the tests conducted.

Table 3 - Beam Designations and Testing Results

Beams	Types of carbon sheets	Total layers	Preloading (kN)
NR	Reference without carbon sheets	0	0
2C1	Reference with two-layer C1	2	0
3C1	Reference with three-layer C1	3	0
1C1C7	Reference with one-layer C1 and one-layer C7	2	0
2C1C7	Reference with two-layer C1 and one-layer C7	3	0
1C1-40	One-layer C1	1	
2C1--40	Two-layer C1	2	40% of steel
3C-1-40	Three-layer C1	3	yielding=14.2
1C1C7-40	One-layer C1 and one-layer C7	2	
1.5C1C7-40	1.5-layer C1 and one-layer C7	2.5	
2C1C7-40	Two-layer C1 and one-layer C7	3	
2C-1-60	Two-layer C1	2	
3C-1-60	Three-layer C1	3	60% of steel
1.5C1C7-60	1.5-layer C1 and one-layer C7	2.5	yielding=21.3
2C1C7-60	Two-layer C1 and one-layer C7	3	

Beams	Maximum load (kN)	Deflection at maximum load (mm)
NR	42.1	19.4
2C1	80.2	20.6
3C1	94.4	13.8
1C1C7	71.2	17.4
2C1C7	88.2	19.4
1C1-40	67.3	18.9
2C1-40	90.9	35.3
3C1-40	90.0	24.5
1C1C7-40	67.2	19.1
1.5C1C7-40	78.7	21.4
2C1C7-40	93.2	30.2
2C1-60	81.9	32.3
3C1-60	88.1	30.7
1.5C1C7-60	69.0	14.3
2C1C7-60	90.9	34.7

The study concluded that the use of these carbon sheets increases flexural stiffness, yielding load and post-yielding ductility. The study also noted no noticeable slope changes in the load-deflection curves at steel yielding which suggested that the beams were stiffened by the hybrid sheets even at steel yield load [11].

Most literature research efforts focus on repairing new beams that are not subjected to any loading; however, in a study titled “Behaviour of preloaded RC beams strengthened with CFRP laminates,” ZHANG Ai-hui et.al [12] performed tests on 18 beams; 2 of which served as control beams and 16 beams were strengthened with bottom CFRP laminates at different preloading levels; the study used preloading stress of 30%, 60% and 80% of nominal beam flexural capacity. The beams were further divided into 2 different categories based on reinforcement ratios and number of plies of CFRP used. The results of the study show that as the level of preloading is increased, the ultimate failure load and ultimate deflection also increase for beams strengthened with one layer of CFRP; for beams strengthened with 2 layers, as the preloading is increased beyond 30%, the ultimate capacity decreases [12].

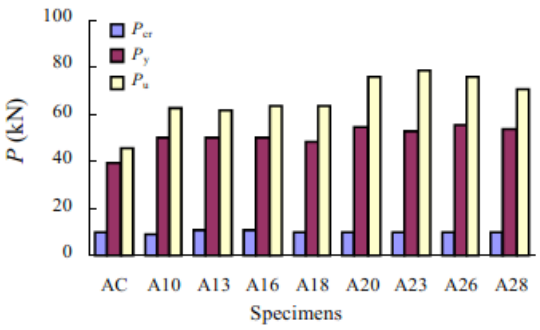

Figure 1 - Comparison of Ultimate Load for all Test Samples [12]

Figure 1 shows a comparison of the ultimate loads in the study. The nomenclature used is in the format of SPL, where S,P,L stand for rebar ratio (2T12 for series A and 2T16 for series B), plies of CFRP (P=1,2) and the preload level (L=0, 3, 6, 8 corresponding to 0, 30%, 60% and 80% of nominal flexural strength of control beams respectively) [12].

Consequently, the importance of the fiber presence in the concrete matrix comes from its ability to increase toughness and improve post-cracking load carrying capacity. Synthetic fibers have relatively high energy-absorption capacity and are resistant to corrosion which makes them ideal for use in concrete matrices. These fibers also improve concrete's resistance to crack development and propagation [12]. Additional research has determined that the larger strength and higher elastic modulus of steel fibers compared to other fibers makes it ideal to be used in hybrid combinations where they contribute to increasing strength and stiffness, in addition to improving the stress for the first crack and the ultimate strength. The presence of another type of fiber, such as synthetic fiber, contributes to bridging micro cracks and reducing crack widths. The more ductile and flexible fibers also improve toughness and strain capacity after concrete has undergone cracking [13]. Therefore, this could contribute to improving the contribution from the external CFRP strengthening.

2.3. ACI-440

ACI-440 code deals with the design equations and criteria for external fiber strengthening of concrete; this includes a variety of material including, but not limited to, carbon, glass and aramid. The ACI-440 code equations do not account for the use of fiber in the concrete mix. Therefore, this study uses the equations in the code to predict

the strength of the strengthened beams and then use them as basis for comparison with the fiber reinforced and preloaded beams.

2.4. Current Practice

The process of strengthening starts by identifying the structural deficiency in the RC member according to which, the orientation and amount of strengthening is determined. The concrete is then grinded to ensure a smooth surface and to remove any unsound concrete for the application of the epoxy; in case of cracked sections, injection of cracks is done before the application of the epoxy. The chemical epoxy is then mixed according to standard proportions and then applied to the surfaces where FRP is to be installed. Finally, the FRP sheets are attached to the beam and the epoxy is left to cure as seen in Figure 2.

Figure 2 – CFRP Installation Process

Chapter 3. Methodology

A total of 15 beams were tested during this study. The beams were casted with different fiber combinations added to the concrete matrix. Following that, the beams were divided into 3 groups –

1. For the first stage, the beams were tested to failure without strengthening or preloading (control samples).
2. For the second stage, the beams were strengthened using CFRP and then tested to failure.
3. For the third stage, the beams were pre-loaded to 67% of the yield strength of the reinforcing steel. The CFRP strengthening was applied after the load is removed. The beams were then tested to failure after complete curing of the CFRP laminates.

The first task included preparing the steel cages, formwork, and required strain gauges for the beams. Figure 3 shows the finished product ready for casting.

Figure 3 - Steel Cages with Formwork and Strain Gauges

The second task involved de-shuttering and curing the beams which was done at the concrete plant. Furthermore, as shown in Figure 4, the third step included preloading the beams from the third stage and preparing them for CFRP installation.

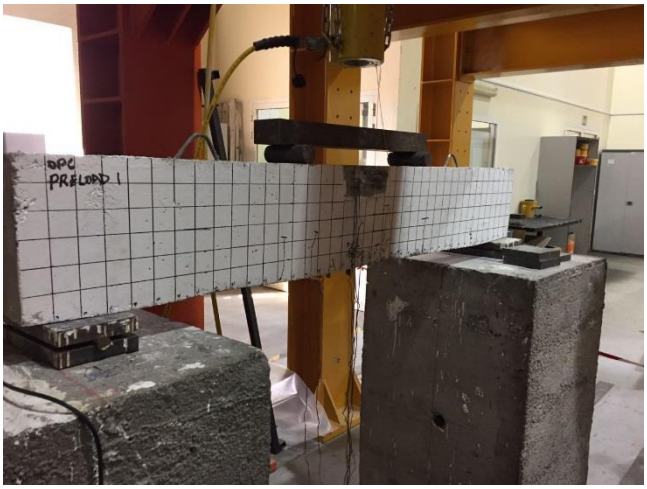

Figure 4 - Preloading Process

The fourth step involved CFRP installation for all the beams and curing the CFRP laminates. Figure 5 shows the beams after being retrofitted with CFRP sheets.

Figure 5 - Finishing CFRP Installation on all Beams

After curing of all CFRP laminates, the beams were tested until failure and all data required was collected using the methods highlighted in chapter 4.

Chapter 4. Experimental Program

The current study is a more realistic representation and estimate in terms of common practices used by repair and strengthening contractors. The strengthening is usually done on RC members that have developed structural deficiencies over time due to exposure or due to a change in the function of the structure.

The evaluation of the effect of CFRP strengthening on the flexural performance of the RC beams was done through bottom side strengthening. A single layer of CFRP was applied to the bottom of the beams along the span.

4.1. Important Parameters

- Beam Size – W x D x L = 150 x 300 x 1800
- CFRP Orientations – Bottom
- 2 T8 Bars for Compression Reinforcement
- Steel Reinforcement –
    - 2 T12 Bars and T10 @ 100mm Stirrups

Preloading Stress Level in flexure steel reinforcement – 310 MPa.

4.2. Material properties

4.2.1. Concrete

Concrete used to cast the beams is C50 with 28-day compressive strength of 50 MPa. Compressive strength was monitored for the concrete used to avoid variations and to verify that the concrete used is of the required strength as shown in Figure 6.

Figure 6 - Compressive Strength Testing

4.2.2. Reinforcement

Steel reinforcement and shear stirrups are hot-rolled deformed rebars of Grade 460 with minimum yield and tensile strengths of 460 and 550 MPa, respectively. The dimensions of the reinforcing steel are displayed in Table 2. Moreover, Figure 7 and Table 4 show the results of testing done on actual steel used; these results are used for theoretical calculations.

Table 4 - Properties of Reinforcing Steel

Type	**Designation**	**Diameter (mm)**	**Area (mm^2)**
Longitudinal Rebar	T8,T12	8,12	50.3,113.1
Stirrups	T10	10	78.5

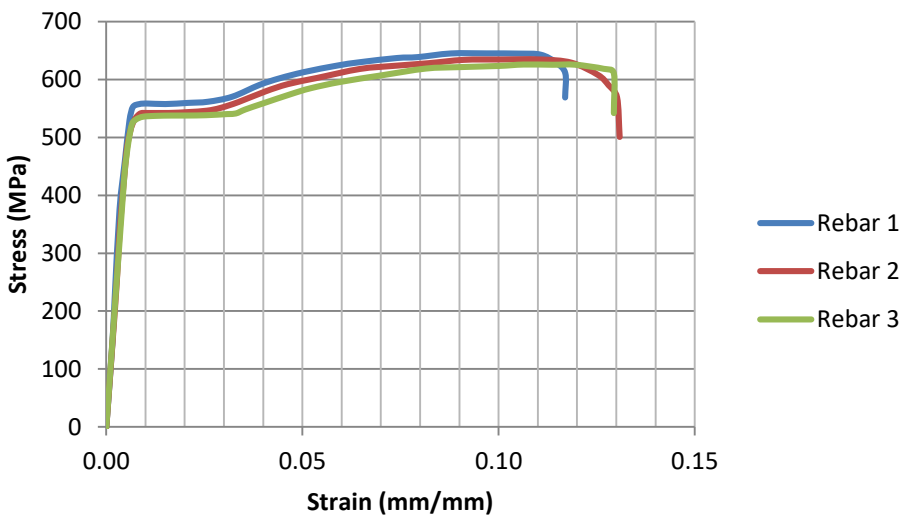

Figure 7 - Stress - Strain Curve for Steel Used

Table 5 - Actual Properties of Steel Used

Specimen	Rebar 1	Rebar 2	Rebar 3	Average
Yield Strength (MPa)	558.35	548.78	547.28	**551.47**
Tensile Strength (MPa)	655.22	633.08	632.21	**640.17**
Modulus of Elasticity (GPa)	199.93	200.01	199.98	**199.97**

4.2.2.1. Steel fiber properties – Dramix 3D

Table 5 summarizes the properties of the steel fiber used; photos of which can be found in appendix A.

Table 6 - Steel Fiber Properties

Properties	Steel Fiber
Length	35mm
Diameter	0.55
Fiber Network	14.531 fibers/kg
Tensile Strength	1345 MPa

4.2.2.2. Synthetic Fiber Properties – STRUX 90/40

Table 6 summarizes the properties of the steel fiber used; photos of which can be found in appendix A.

Table 7 - Synthetic Fiber Properties

Properties	**Steel Fiber**
Specific Gravity	0.92
Absorption	None
Modulus of Elasticity	9.5 GPa
Tensile Strength	620 MPa
Melting Point	160 Degrees
Ignition Point	590 Degrees

4.2.2.3. V-wrap C200H (CFRP sheets)

Tables 8 and 9 show the relevant dry and cured properties of the CFRP laminates used. Additionally, Figure 8 shows the stress-strain behaviour of CFRP laminates when compared to GFRP and Mild Steel. The CFRP has higher stress for the same strain value compared to GFRP and steel, however, CFRP is not ductile compared to steel.

Table 8 - Fiber Properties (Dry)

Tensile Strength (MPa)	4820
Tensile Modulus (GPa)	27.6
Elongation (%)	1.7

Table 9 - Cured Laminate Properties

	Average Value	Design Value
Tensile Strength (MPa)	1,240	1,030
Modulus of Elasticity (GPa)	91.7	82.7
Elongation at Break (%)	1.35	1.25
Thickness (mm)	1.27	1.27
Strength per Inch Width (kN/layer)	40.0	33.3

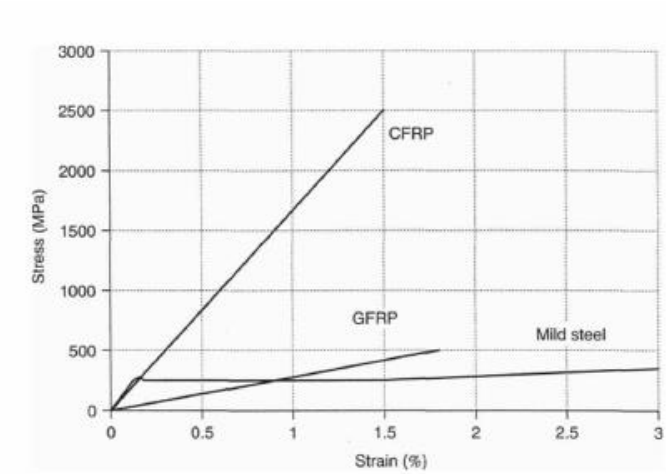

Figure 8 - Stress-Strain Behavior of CFRP vs. GFRP and Mild Steel [15]

In this study, the effect of CFRP strengthening on the flexural performance of preloaded fiber reinforced concrete beams were studied. The repair was done to model real life conditions where the steel rebars are exposed to loading conditions throughout the life of the structure before introducing the need for repair. Preloading is expected to contribute to initiation of cracks in the concrete microstructure and also might affect the bond between the concrete and steel rebar. Theoretically, the contribution of CFRP strengthening might vary depending on the level of cracks and loss of bond. The reinforcement ratio of 0.55% is used in this study to be compared to the literature.

Figure 9 shows the cross sectional details of the beams in the study.

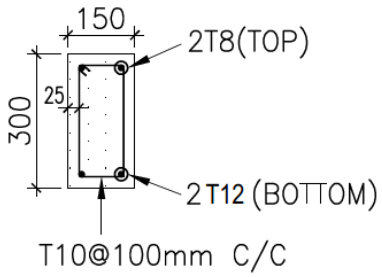

Figure 9 - Cross Section Details of Study Beams

For the purpose of this study, CFRP Strengthening orientation is as follows–

- Bottom CFRP Sheets were used to increase the flexural capacity of the beam; for that purpose, the beam is adequately reinforced with stirrups to avoid introduction of shear failure during testing.

The study beam elevation in Figure 10 is shown where 4-point loading was used to create a region of maximum moment in the middle 0.6 m portion of the beam.

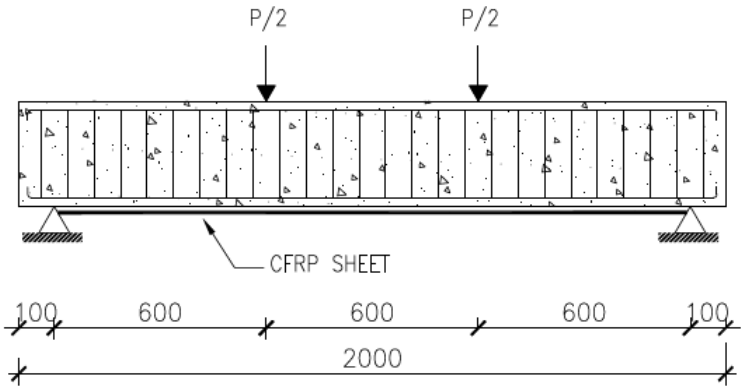

Figure 10 - Elevation View of Study Beam with Loading

4.3. Test Setup

Figure 11 shows the test setup used in testing all beams during this study. The setup consists of a hydraulic jack; a load cell to monitor and record the load, position transducer to monitor the deflection, in addition, strain gauges were used to measure the strain in the steel, concrete and the FRP sheets.

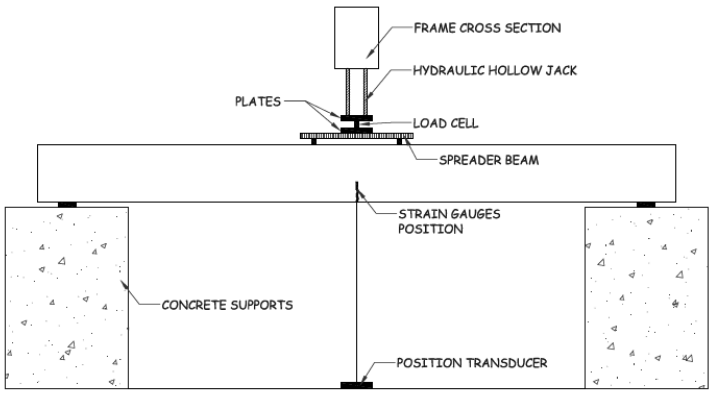

Figure 11 - Test Setup and instrumentations

Table 10 provides information about the samples that were cast along with the different parameters that were varied.

Table 10 - Summary of Samples for Experimental Program

	Plain	**Steel Fiber**	**Synthetic Fiber**	**Hybrid**
Control	1	1	1	1
Strengthened	1	1	1	1
Preloaded	2	2	2	1

Chapter 5. Results and Analysis

5.1. Results of Experimental Investigation

In this chapter, results of tests conducted will be reported in tabular and graphical representation. Table 9 summarizes test results of all beams. First Crack Load (kN), Strain at First Crack, Load at Yield (kN), Maximum Load (kN), Max. Deflection (mm), and Mode of Failure are listed for comparison.

Table 11 – Summary of Results from Experimental Investigation

Beam ID	First Crack Load (kN)	Strain at First Crack	Load at Yield (kN)	Maximum Load (kN)	Max. Deflection (mm)	Mode of Failure
Plain Control	35	802	74.61	117.43	14.96	Flexural Failure
Steel Fiber Control	32	811	99.21	192.73	20.71	Flexural Failure
% Increase*	-9%	1%	33%	64%	38%	
Synthetic Fiber Control	46	767	112.34	190.43	27.07	Flexural Failure
% Increase*	31%	-4%	51%	62%	81%	
Hybrid Control	39	1404	113.52	200.21	22.26	Flexural Failure
% Increase*	11%	75%	52%	70%	49%	
Plain Strengthened	49	1176	121.78	196.35	13.97	Delamination
Steel Fiber Strengthened	80	1137	134.79	257.51	18.04	Delamination
% Increase**	63%	-3%	11%	31%	29%	
Synthetic Fiber Strengthened	91	1237	154.82	241.84	27.68	Delamination
% Increase**	86%	5%	27%	23%	98%	
Hybrid Strengthened	86	1156	143.55	272.71	20.15	Delamination
% Increase**	76%	-2%	18%	39%	44%	
Plain Preloaded 1	53	420	161.24	249.97	17.63	Delamination
Plain Preloaded 2	65	538	157.62	271.33	16.59	Delamination
Steel Fiber Preloaded 1	65	1273	142.12	287.85	27.16	Delamination
Steel Fiber Preloaded 2	67	1127	139.92	256.71	20.21	Delamination
Average % Increase***	12%	151%	-12%	4%	38%	
Synthetic Fiber Preloaded 1	60	1482	158.47	273.57	28.97	Delamination
Synthetic Fiber Preloaded 2	70	1029	132.26	213.23	12.28	Delamination
Average % Increase***	10%	162%	-9%	-7%	21%	
Hybrid Preloaded 1	86	972	144.31	298.33	19.65	Delamination
% Increase***	46%	103%	-9%	14%	15%	

*Compared to Plain Control **Compared to Plain Strengthened ***Compared to Plain Preloaded

First crack load is an important parameter to determine the effect of fiber addition, strengthening and preloading on the cracking moment of the beam. The load at yield is also important in determining the efficiency of the strengthening method to cause an increase in the load at yield. Additionally, the two most important results of this study were the maximum load that the beam can take along with the maximum deflection which gives an idea about the ductility of the beam; these parameters were critical as they provide basis for comparison between the different concrete matrices and strengthening techniques used in this study. Furthermore, the observed mode of failure was flexural failure for all control beams and delamination for all CFRP strengthened beams as shown in Figures 12, 13, 14, and 15. Additional photos of failure modes for tested beams can be found in Appendix B.

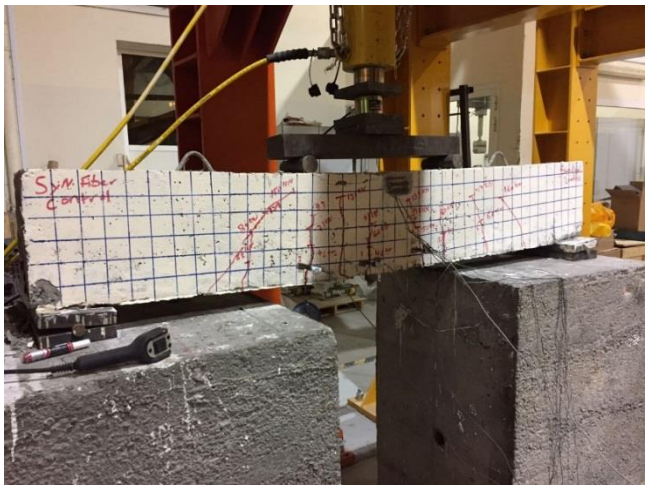

Figure 12 - Flexural Failure of Synthetic Fiber Control Beam

Figure 13 - Delamination Failure of Strengthened Beam

Figure 14 - Delamination Failure of Strengthened Beams

Figure 15 - Delamination Failure

5.2. Load-Deflection Results for Control Beams

The graphs in Figure 18 show the raw test data plotted on the same graph along with digitized plots that have been created for the same set of data. It is prevalent that both the curves are very close to each other and therefore, only the digitized plots will be used for discussion.

Additionally, figure 16 shows the load-deflection curves for all control beams. The test results showed that the addition of synthetic fiber, fig. 18c, greatly improves the ductility of the beam; this is characterized by the value of maximum deflection obtained for all tested beams.

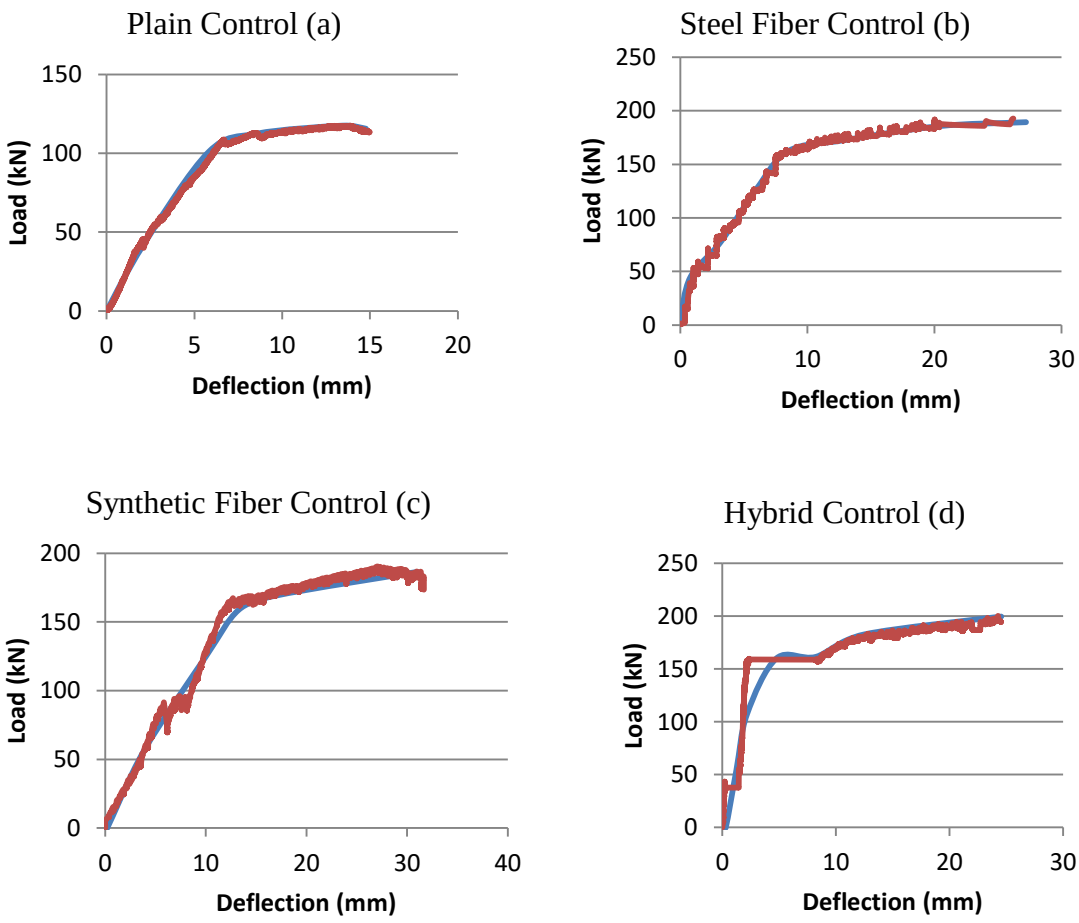

Figure 16 - Load-Deflection Curves for Control Beams

5.3. Load-Deflection Results for Strengthened Beams

Figure 17 shows the load-deflection curves for all strengthened beams. The application of CFRP greatly increases the flexural strength of the beam. Additionally, similar to the behaviour of control beams, the synthetic fiber, fig. 19 c, greatly improves the ductility of the beam.

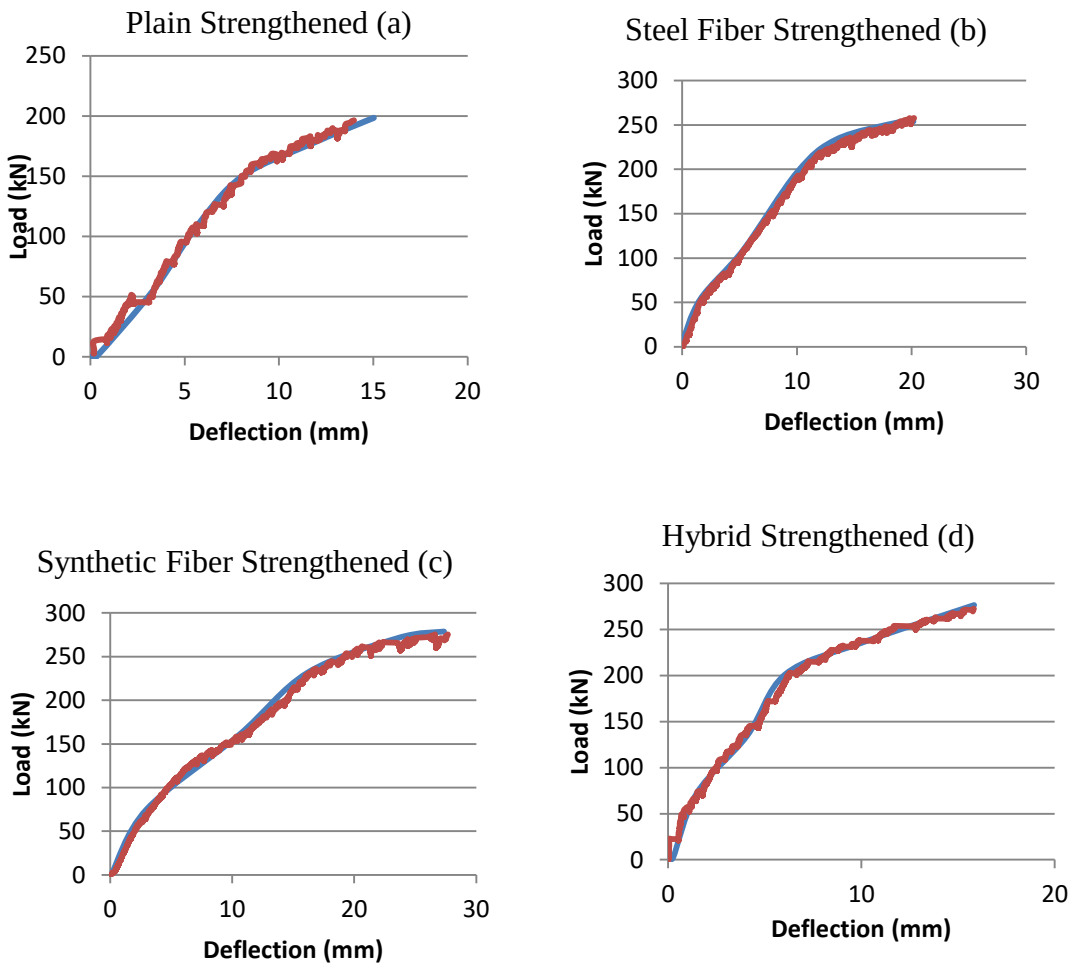

Figure 17- Load-Deflection Curves for Strengthened Beams

5.4. Load-Deflection Curves for Preloaded Beam

Figure 18 shows the load-deflection curves for all preloaded beams. The preloading process has increased the ultimate capacity and contribution from the CFRP and resulted in higher ultimate strength and greater ductility.

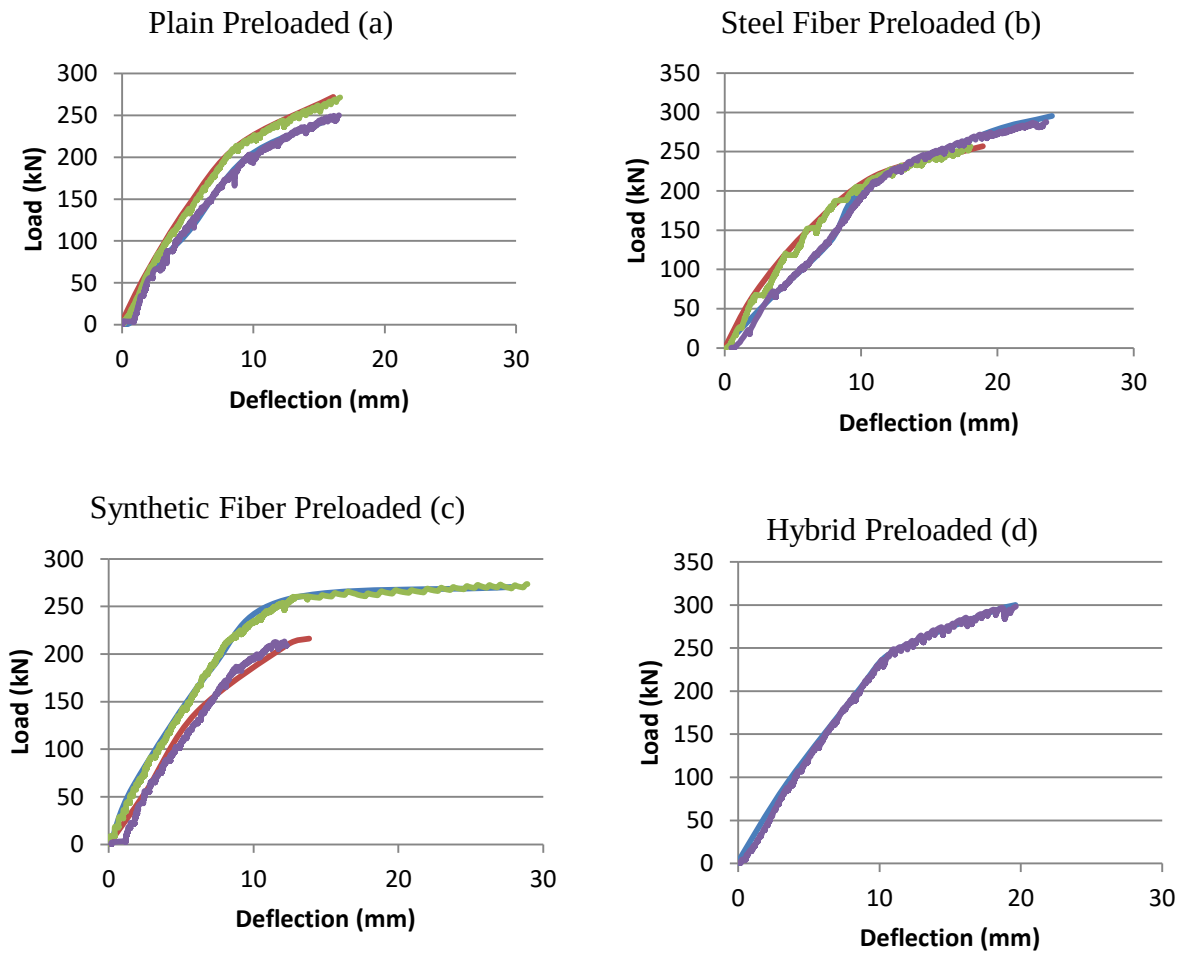

Figure 18 - Load-Deflection Curves for Preloaded Beams

5.5. Cracking Load for First Five Cracks

Table 12 summarizes the cracking loads for the first five cracks for all the tested beams; the cracks were carefully monitored as the load was gradually increased using the load cell.

Table 12 - Crack Loads for First Five Cracks

`Beam ID	Crack 1 Load (kN)	Crack 2 Load (kN)	Crack 3 Load (kN)	Crack 4 Load (kN)	Crack 5 Load (kN)
Plain Control	35	39	41	48	55
Steel Fiber Control	32	53	55	68	74
Synthetic Fiber Control	46	46	59	66	66
Hybrid Control	39	53	53	59	60
Plain Strengthened	49	49	49	54	60
Steel Fiber Strengthened	80	80	82	95	99
Synthetic Fiber Strengthened	91	108	127	145	184
Hybrid Strengthened	86	88	92	93	97
Plain Preloaded 1	53	69	83	112	114
Plain Preloaded 2	65	68	68	85	112
Steel Fiber Preloaded 1	65	65	65	81	102
Steel Fiber Preloaded 2	67	71	72	88	97
Synthetic Fiber Preloaded 1	60	80	88	110	115
Synthetic Fiber Preloaded 2	70	70	70	79	89
Hybrid Preloaded 1	86	92	92	117	134

5.6. Effect of Preloading on CFRP Contribution

Table 13 and Figure 19 summarize the results for all the plain test samples from the experimental investigation and highlight the effect of CFRP strengthening, with and without preloading, on the behaviour of the beam. In the case of absence of fibers, the un-strengthened beam showed a very early first crack at 35 kN and had the lowest load-capacity at 117.43 kN. The application of CFRP to the plain beam caused a 40% increase in first crack load and a 68% increase in the beam's ultimate carrying capacity due to the contribution of CFRP towards increasing the overall stiffness of the beam, which is displayed through the higher initial slope of the load-deflection graphs, and acting as external reinforcement. Furthermore, the preloaded beams, which have been strengthened after undergoing a preload to 0.67Fy at reinforcement steel level, displayed a 33% average increase in the ultimate load carrying capacity which is attributed to the fact that preloading initiates the cracking process and when the CFRP is applied to the crack member, it is engaged immediately and gives a higher contribution. Additionally, a very important benefit of strengthening after preloading was a 22% and 14% increase in maximum deformation when compared to beams that have been strengthened without preloading and beams that have not been strengthened, respectively. Strengthening also delayed the yielding of the steel by 63% of the load due to an increase in the effective area of tension reinforcement which brings the section behaviour closer to that of an overly-reinforced member.

Table 13 - Comparison between Plain Test Samples

Beam ID	First Crack Load (kN)	Strain at First Crack	Load at Yield (kN)	Maximum Load (kN)	Strain at Max. Load	Max. Deflection (mm)	Mode of Failure
Plain Control	35	802	74.61	117.43	3935	14.96	Flexural Failure
Plain Strengthened	49	1176	121.78	196.35	4891	13.97	Delamination
Plain Preloaded	65	538	157.62	271.33	8652	16.59	Delamination

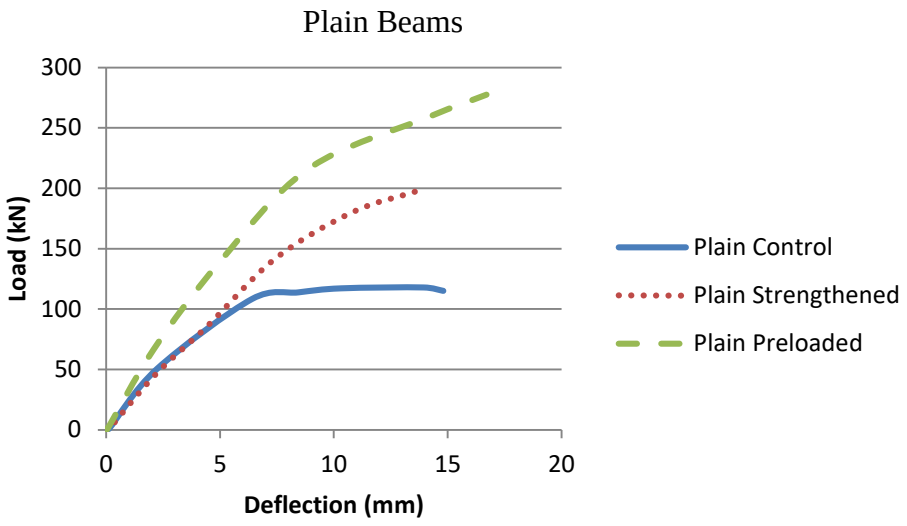

Figure 19 - Comparison between Plain Test Samples

Table 14 and Figure 20 summarize the results for all the steel fiber reinforced test samples from the experimental investigation and highlight the effect of CFRP strengthening, with and without preloading, on the behaviour of the beam with steel fiber incorporated into the mix. The steel fiber control beam showed a relatively early first crack initiation; this is attributed to the fact that steel fiber mainly contributes to the flexural capacity of the beam rather than add ductility and prevent crack mitigation [16]. Similar to the behaviour in the case of the plain samples, the strengthened beam showed had a 13% reduction in maximum deflection; the strengthened beam also showed a 33% increase in maximum load which are both attributed to the higher stiffness shown in the initial slope of the curves in Figure 22. Furthermore, the preloaded beams showed a 13% increase in maximum deflection; the preloaded beam also caused a 41% and 6% increase in strength when compared to the un-strengthened and strengthened beams respectively. The strengthening also caused a 36% increase in the yield load of the steel reinforcement justified by the additional reinforcement that reduces the strain in the steel reinforcement at a particular load.

Table 14 - Comparison between Steel Fiber Test Samples

Beam ID	First Crack Load (kN)	Strain at First Crack	Load at Yield (kN)	Maximum Load (kN)	Strain at Max. Load	Max. Deflection (mm)	Mode of Failure
Steel Fiber Control	32	811	99.21	192.73	5062	20.71	Flexural Failure
Steel Fiber Strengthened	80	1137	134.79	257.51	2998	18.04	Delamination
Steel Fiber Preloaded	65	1273	142.12	287.85	5983	27.16	Delamination

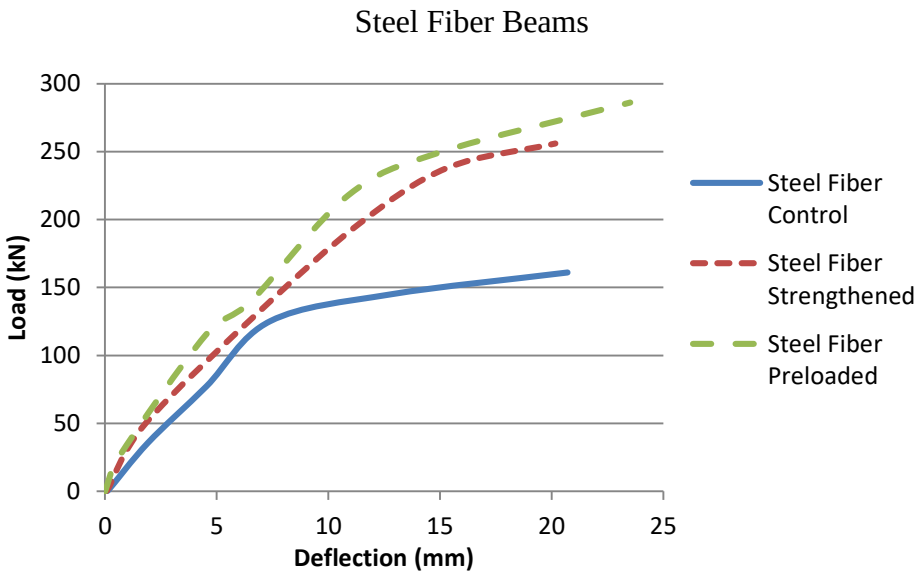

Figure 20 - Comparison between Steel Fiber Test Samples

Table 15 and Figure 21 summarize the results for all the synthetic fiber reinforced test samples from the experimental investigation and highlights the effect of CFRP strengthening, with and without preloading, on the behaviour of the beam with synthetic fiber incorporated into the mix. Beams reinforced with synthetic fiber had higher ductility and first crack initiation load; the beam also had relatively high maximum deflection without any strengthening which is attributed to the high energy absorption of the synthetic fibers which delays initial cracking and makes the cracks smaller; this confirms the efficiency of synthetic fibre in increasing the beam's resistance to crack development and propagation. [13] In the case of synthetic fiber, the strengthening caused a 12% reduction in maximum deflection but caused a 27%

increase in the maximum load taken. The CFRP strengthening contributed to increase the steel yield load by 41%.

Table 15 - Comparison between Synthetic Fiber Test Samples

Beam ID	First Crack Load (kN)	Strain at First Crack	Load at Yield (kN)	Maximum Load (kN)	Strain at Max. Load	Max. Deflection (mm)	Mode of Failure
Synthetic Fiber Control	46	767	112.34	190.43	8959	27.07	Flexural Failure
Synthetic Fiber Strengthened	91	1237	154.82	241.84	2934	27.68	Delamination
Synthetic Fiber Preloaded 1	60	1482	158.47	273.57	2792	28.97	Delamination

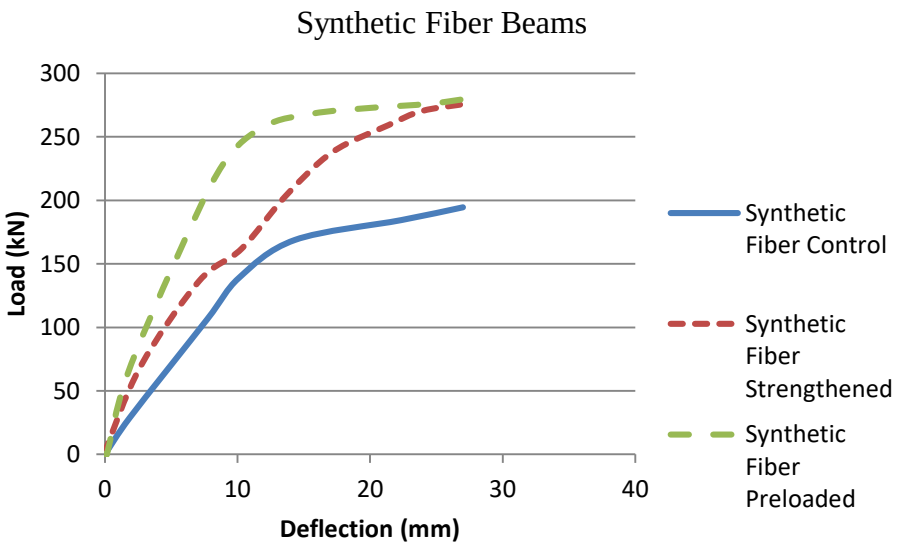

Figure 21 - Comparison between Synthetic Fiber Test Samples

Table 16 and Figure 22 summarize the results for all the hybrid fiber reinforced test samples from the experimental investigation and highlights the effect of CFRP strengthening, with and without preloading. In the case of hybrid fiber, the maximum deflection values are within 10% of each other and no apparent trend is observed. However, the presence of fiber greatly affects the maximum load and causes an increase of 36% and 49% in the case of strengthened and preloaded beams, respectively. It is prevalent that the steel fiber dominates the contribution of the hybrid mix and the

replacement percentages should consider the difference in stiffness, elastic modulus and density of both fibers.

Table 16 - Comparison between Hybrid Test Samples

Beam ID	First Crack Load (kN)	Strain at First Crack	Load at Yield (kN)	Maximum Load (kN)	Strain at Max. Load	Max. Deflection (mm)	Mode of Failure
Hybrid Control	39	1404	78.11	200.21	5500	22.26	Flexural Failure
Hybrid Strengthened	86	1156	143.55	272.71	7281	20.15	Delamination
Hybrid Preloaded	86	972	144.31	298.33	4632	19.65	Delamination

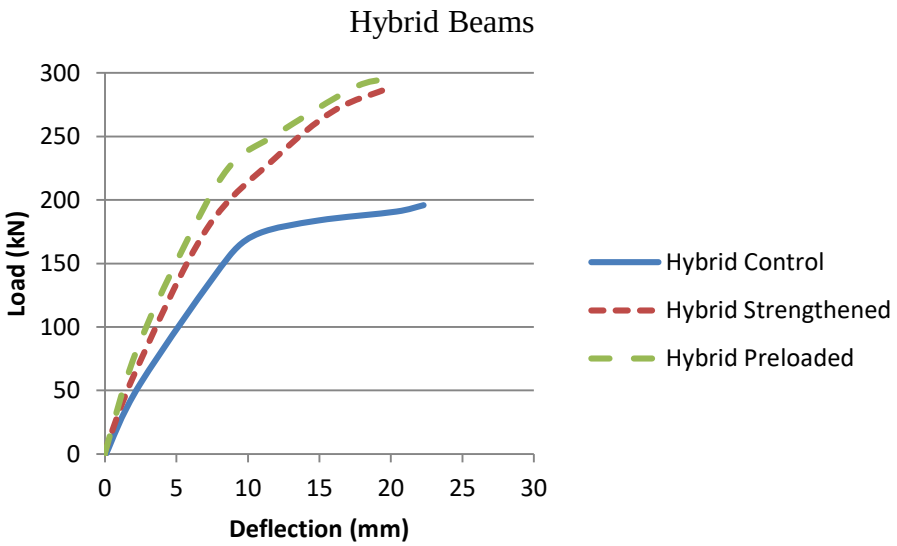

Figure 22 - Comparison between Hybrid Test Samples

Table 17 and Figure 23 summarize the differences caused by the addition of different types of fibers to the concrete matrix. The addition of steel fiber has very little influence on the first crack load; however, synthetic fibers are more effective in delaying the cracking process due to their distribution and flexibility that allows them to bridge the small cracks and prevent their mitigation. Additionally, the addition of fiber greatly improves the load-carrying capacity of the concrete beams; steel fiber increases the capacity by 64% and the synthetic fiber increases the capacity by 61%. In terms of ductility, steel fiber has almost no effect on maximum deflection; it causes a

7% reduction in maximum deflection when compared to the control beam which can be overlooked since it is within 10%. On the other hand, synthetic fibers caused a 42% increase in maximum deflection due to their high energy absorption and ability to significantly increase ductility. The mix containing the hybrid mix of fibers displays characteristics of both steel and synthetic fibers; it causes a 70% increase in strength and a 9% increase in maximum deflection when compared to the control beam. Similar to the previous discussion, the effect of steel fiber is more prevalent in the hybrid beam due to their higher stiffness and elastic modulus.

Table 17 - Comparison between Control Test Samples

Beam ID	First Crack Load (kN)	Strain at First Crack	Load at Yield (kN)	Maximum Load (kN)	Strain at Max. Load	Max. Deflection (mm)	Mode of Failure
Plain Control	35	802	74.61	117.43	3935	14.96	Flexural Failure
Steel Fiber Control	32	811	99.21	192.73	5062	20.71	Flexural Failure
Synthetic Fiber Control	46	767	112.34	190.43	8959	27.07	Flexural Failure
Hybrid Control	39	1404	78.11	200.21	5500	24.26	Flexural Failure

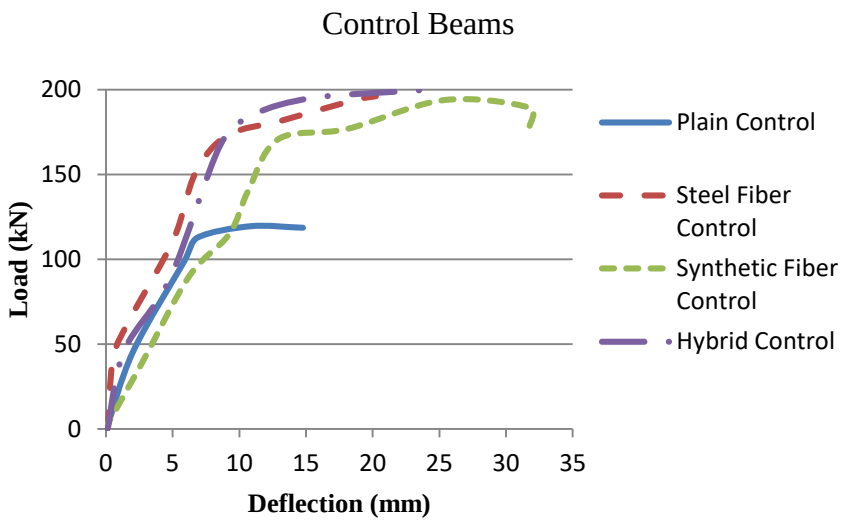

Figure 23 - Comparison between Control Test Samples

Figure 24 shows a comparison between theoretical capacity and actual capacity of all tested beams; the addition of fiber noticeably increases the ultimate moment capacity of the section. The detailed calculations can be found attached in Appendix C.

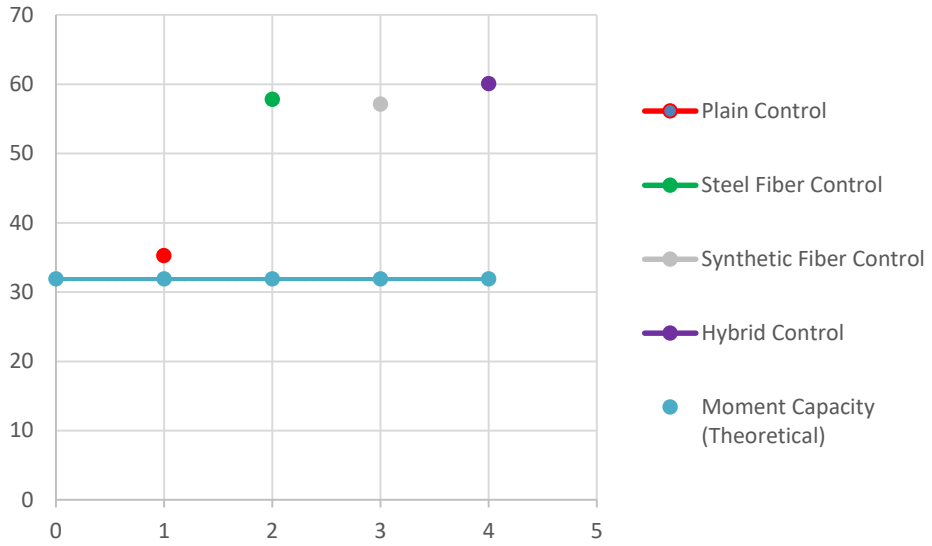

Figure 24 - Comparison between Ultimate Capacities of Beams vs Theoretical

Table 18 and Figure 25 show the effect of CFRP strengthening on beams containing different types of fibers in the mix. The effect of strengthening on the first cracking load is significant; there is a 63%, 85% and 76% increase in crack initiation load in the cases of steel fiber, synthetic fiber and hybrid mix of fibers, respectively. Additionally, strengthening causes 31%, 23% and 39% increase in maximum load for the fiber strengthened beams. In terms of deflection, the effect of strengthening is greatly affected by the type of fiber in the mix; the increase in maximum deflection when compared to the control beams without fiber are 29%, 98% and 14% for steel, synthetic and hybrid fiber reinforced beams, respectively.

Table 18 - Comparison between Strengthened Test Samples

Beam ID	First Crack Load (kN)	Strain at First Crack	Load at Yield (kN)	Maximum Load (kN)	Strain at Max. Load	Max. Deflection (mm)	Mode of Failure
Plain Strengthened	49	1176	121.78	196.35	4891	13.97	Delamination
Steel Fiber Strengthened	80	1137	134.79	257.51	2998	18.04	Delamination
Synthetic Fiber Strengthened	91	1237	154.82	241.84	2934	27.68	Delamination
Hybrid Strengthened	86	1156	143.55	272.71	7281	20.15	Delamination

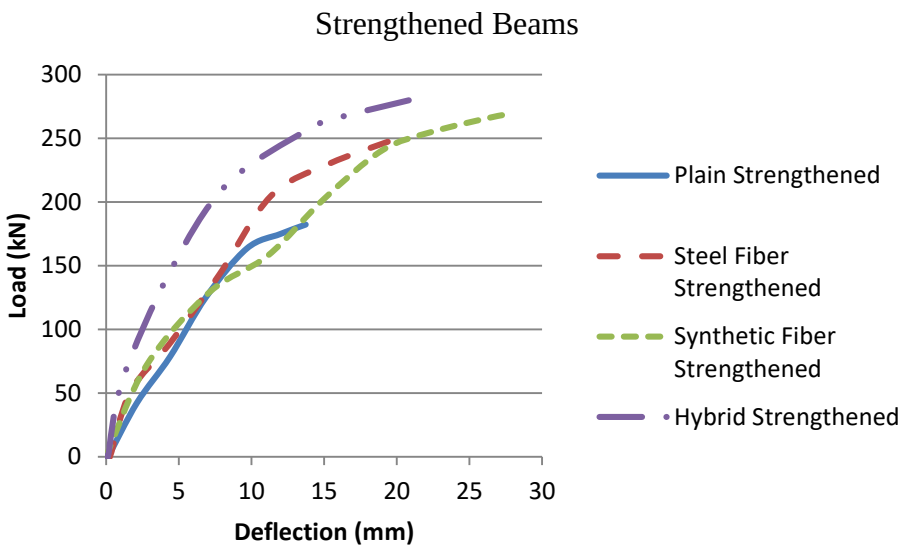

Figure 25 - Comparison between Strengthened Test Samples

Table 19 and Figure 26 summarize the effect of preloading on the beams containing different fiber types. Preloading overall increases the maximum load the beam can carry. Additionally, as in previous cases, synthetic fiber beams had the highest maximum deflection; the maximum deflection was 75% more than the plain preloaded beam. The highest additional capacity was observed in the hybrid fiber strengthened beams with a 10% increase in maximum load when compared to the plain preloaded beam.

Table 19 - Comparison between Preloaded Test Samples

Beam ID	First Crack Load (kN)	Strain at First Crack	Load at Yield (kN)	Maximum Load (kN)	Strain at Max. Load	Max. Deflection (mm)	Mode of Failure
Plain Preloaded	65	538	157.62	271.33	8652	16.59	Delamination
Steel Fiber Preloaded	65	1273	142.12	287.85	5983	22.65	Delamination
Synthetic Fiber Preloaded	60	1482	158.47	273.57	2792	28.97	Delamination
Hybrid Preloaded	86	972	144.31	298.33	4632	19.65	Delamination

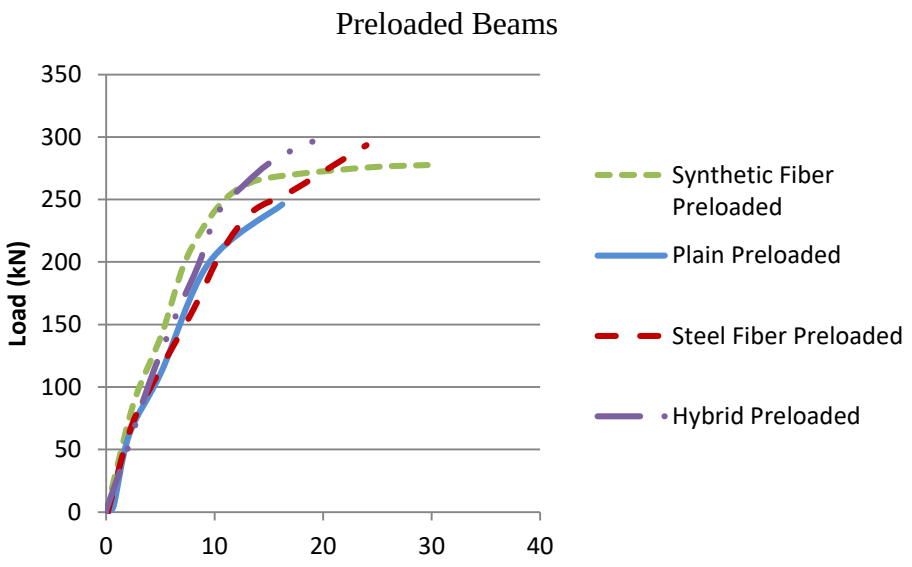

Figure 26 - Comparison between Preloaded Test Samples

Figure 27 shows a comparison between the moment capacities of the tested beams and the theoretical capacity predicted using the ACI-440. Preloading has shown to have achieved higher capacities when compared to the beams that were strengthened but not preloaded. Additionally, the addition of fiber has caused an increase in the flexural strength of all beams compared to the control calculations; detailed calculation can be found in Appendix D.

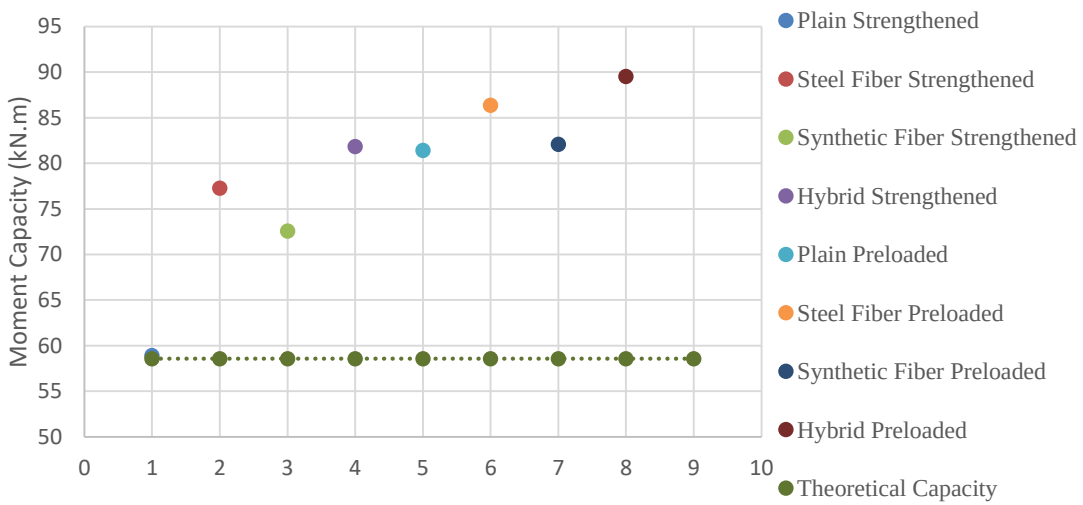

Figure 27 - Comparison between Strengthened/Preloaded Beams and Theoretical Capacity

Table 20 summarizes the cracking loads for the first 5 cracks for all the test beams. As shown, the plain control and steel fiber control have the lowest crack initiation loads. It is noticeable that the addition of fiber and strengthening significantly contribute to the crack initiation load of the beams; this is because steel fiber increase the flexural capacity of the beam and synthetic fiber act as crack bridges which prevents their early mitigation. The strengthened beam with synthetic fiber showed the greatest increase in first crack load by 184% when compared to the steel fiber control.

Table 20 - Summary of Loads for First 5 Cracks for Test Beams

`Beam ID	Crack 1 Load (kN)	Crack 2 Load (kN)	Crack 3 Load (kN)	Crack 4 Load (kN)	Crack 5 Load (kN)
Plain Control	35	39	41	48	55
Steel Fiber Control	32	53	55	68	74
Synthetic Fiber Control	46	46	59	66	66
Hybrid Control	39	53	53	59	60
Plain Strengthened	49	49	49	54	60
Steel Fiber Strengthened	80	80	82	95	99
Synthetic Fiber Strengthened	91	108	127	145	184
Hybrid Strengthened	86	88	92	93	97
Plain Preloaded 1	53	69	83	112	114
Plain Preloaded 2	65	68	68	85	112
Steel Fiber Preloaded 1	65	65	65	81	102
Steel Fiber Preloaded 2	67	71	72	88	97
Synthetic Fiber Preloaded 1	60	80	88	110	115
Synthetic Fiber Preloaded 2	70	70	70	79	89
Hybrid Preloaded 1	86	92	92	117	134

Chapter 6. Conclusion and Future Work

In this thesis, steel, synthetic and hybrid fibers were introduced to concrete mixes to evaluate the effect of fiber addition on the flexural strength of reinforced concrete beams. Moreover, CFRP strengthening was applied to the casted beams in two groups; the first group had strengthening done on the freshly casted beam after completing curing period and the second group was preloaded to 67% of yield stress of the steel and then strengthened with CFRP. In conclusion, the addition of fiber greatly affects mechanical and durability performance of reinforced concrete; the addition of steel fiber increases the flexural capacity of the beam. On the other hand, the addition of synthetic fiber has no noticeable effect on the flexural capacity of the beam but greatly increase the beam's ductility and improves the post cracking behaviour. Furthermore, preloading the concrete beams before strengthening resulted in improved ductility and higher strength when compared to the beams that were not preloaded; this can be attributed to the fact that preloading initiates the cracking process in the beam and therefore, when the CFRP is applied and beam is tested until failure, the CFRP sheets are engaged earlier and show higher contribution towards the strength of the beam. Another justification is that, when the beams that have not been preloaded are strengthened and tested, the crack initiation process creates stress concentrations at those locations which reduces the effectiveness of the CFRP strengthening.

Additionally, it has been observed that beams strengthened with synthetic fiber experience smaller but more frequent cracking under loading due to the high energy-absorption capacity of the synthetic fiber.

As a recommendation for future work, the beams could be preloaded up to the yield stress of the steel reinforcement. Another approach would be to strengthen the beams under loading and compare them to beams that have been preloaded and repaired after the load was removed. Additionally, using different steel reinforcement ratios could be a good approach towards building on the work done in this thesis.

References

[1] O. Rabinovitch and Y. Frostig, 'Experiments and analytical comparison of RC beams strengthened with CFRP composites', Composites, no. 34, pp. 663-677, 2003.

[2] A. El-Shihy, H. Shehab, and M. Mansour, “Repair and Renovation of Concrete Structures,” in *Repair and Renovation of Concrete Structures*, 2005.

[3] H. Allam and M. Hosein, 'Strengthening of Loaded Beams by CFRP', in The third Middle East symposium on structural composites for infra-structure applications, Aswan, 2002, pp. 135-137.

[4] Qingxin Zhao, Junchao Yu, Guoqing Geng, Jinyang Jiang, Xiaochen Liu, Effect of fiber types on creep behavior of concrete, Construction and Building Materials, Volume 105, 15 February 2016, Pages 416-422, ISSN 0950-0618, http://dx.doi.org/10.1016/j.conbuildmat.2015.12.149.

[5] Balaguru P., Nanni A, and Giancaspro “FRP Composites for RC and PC Structures” 2009, Taylor and Francis

[6] H. Kim and Y. Shin, 'Flexural Behavior of reinforced concrete (RC) beams retrofitted with hybrid fiber reinforced polymers (FRPs) under sustaining loads', Composite Structures, vol. 93, pp. 802-811, 2010.

[7] I. Jankowiak, 'Analysis of RC beams strengthened by CFRP strips - Experimental and FEA study', Archives of Civil and Mechanical Engineering, pp. 376-388, 2012.

[8] J.A.O. Barros, S.J.E. Dias and J.L.T. Lima, 'Efficacy of CFRP-based techniques for the flexural and shear strengthening of concrete beams', Cement & Concrete Composites, pp. 203-217, 2006.

[9] R. Hawileh, H. Rasheed, J. Abdalla and A. Al-Tamimi, 'Behavior of reinforced concrete beams strengthened with externally bonded hybrid fiber reinforced polymer systems', Materials and Design, pp. 972-982, 2013.

[10] N. Attari, S. Amziane and M. Chemrouk, 'Flexural strengthening of concrete beams using CFRP, GFRP and hybrid FRP sheets', Construction and Building Materials, no. 37, pp. 746-757, 2012.

[11] Z. Wu, Y. Shao, K. Iwashita, and K. Sakamoto, “Strengthening of Preloaded RC Beams Using Hybrid Carbon Sheets,” Journal of Composites for Construction, ASCE, vol. 11, no. 3, pp. 299–307, Jun. 2007.

[12] A.-H. Zhang, W.-L. Jin, and G.-B. Li, “Behavior of preloaded RC beams strengthened with CFRP laminates,” Journal of Zhejiang University-SCIENCE A, vol. 7, no. 3, pp. 436–444, 2006.

[13] B. Hwan Oh, D. Park, J. Kim and Y. Choi, "Experimental and theoretical investigation on the postcracking inelastic behavior of synthetic fiber reinforced concrete beams", Cement and Concrete Research, vol. 35, no. 2, pp. 384-392, 2005.

[14] E. Dawood and M. Ramli, "Durability of high strength flowing concrete with hybrid fibres", Construction and Building Materials, vol. 35, pp. 521-530, 2012.

[15] R. Benzaid and H.-A. Mesbah, “Circular and Square Concrete Columns Externally Confined by CFRP Composite: Experimental Investigation and Effective Strength Models,” Fiber Reinforced Polymers - The Technology Applied for Concrete Repair, 2013.

[16] S. Yehia, A. Douba, O. Abdullahi, and S. Farrag, “Mechanical and durability evaluation of fiber-reinforced self-comapacting concrete,” Construction and Building Materials, pp. 120–133, Jun. 2016.

APPENDICES

APPENDIX A - MATERIALS

Figure A1 – Steel Fibers Used

Figure A2 – Synthetic Fibers Used

APPENDIX B – FAILURE MODES

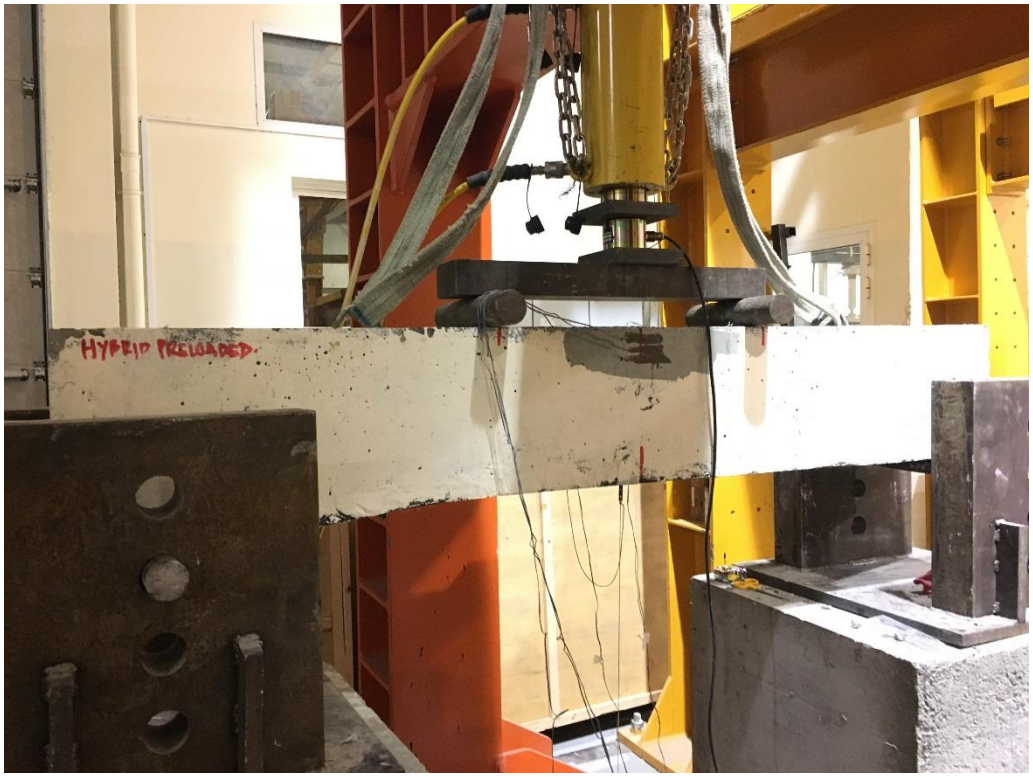

Figure A3 – Test Setup

Figure A4 – Post Failure of Hybrid Preloaded Beam

Figure A5 – Post Failure of Plain Preloaded Beam

Figure A6 – Post Failure of Steel Fiber Strengthened Beam

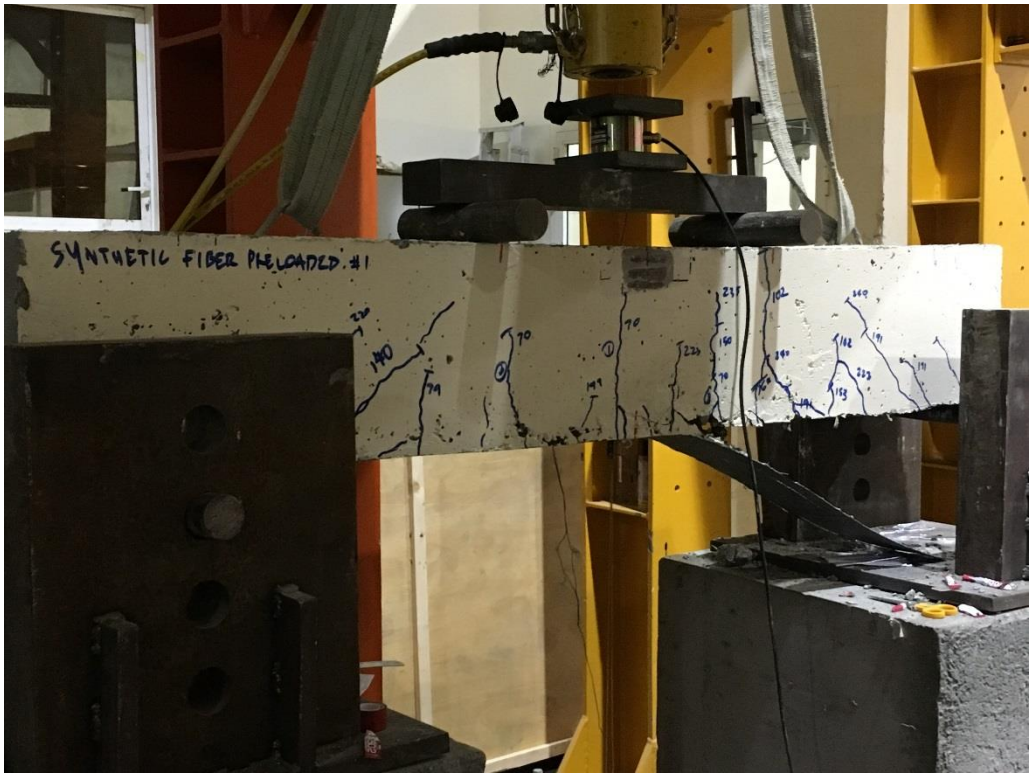

Figure A7 – Post Failure of Synthetic Fiber Preloaded Beam

Figure A8 – Post Failure of Plain Strengthened Beam

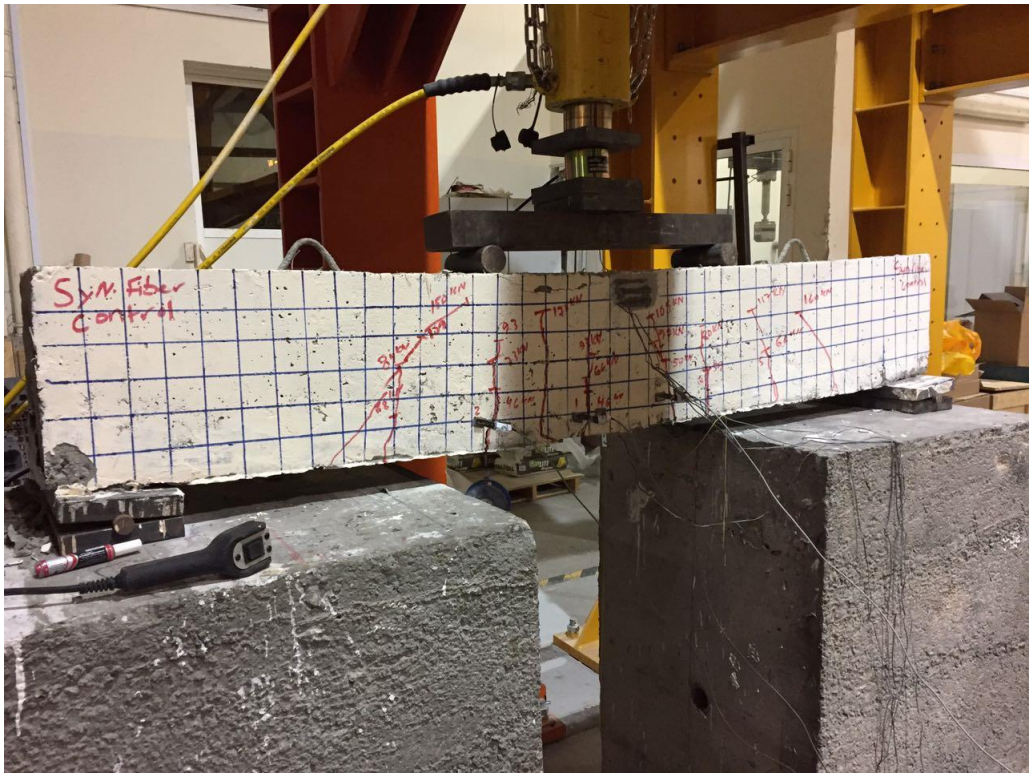

Figure A9 – Post Failure of Synthetic Fiber Control Beam

APPENDIX C – CONTROL CALCULATIONS

Flexural Strengthening Design - SI Units
ACI 318-08

STRUCTURAL TECHNOLOGIES
7455-T New Ridge Road
Hanover, MD 21076-3143 USA
Tel: 410-850-7000 Fax: 410-850-4111
www.structural.net

Project: Masters Thesis

Condition: Control Beam

Level: ---

Designed by: KH

Date: 17th April, 2017

Required Information about the Existing Structure

Section Dimensions

$h := 300$	Total section height [mm]
$bw := 150$	Width of web [mm]
$bft := 0$	Width of top flange (zero for rectangular or inverted tee sections) [mm]
$tft := 0$	Thickness of top flange (zero for rectangular or inverted tee sections) [mm]
$bfb := 0$	Width of bottom flange (zero for rectangular or tee sections) [mm]
$tfb := 0$	Thickness of bottom flange (zero for rectangular or tee sections) [mm]

Reinforcement Layout

$As := 2 \cdot 113$	Area of mild tension steel [mm^2]
$d := h - 30$	Depth to the mild tension steel centroid [mm]
$As2 := 0$	Second Area of mild tension steel [mm^2]
$d2 := d$	Depth to the second mild tension steel centroid [mm]
$As' := 2 \cdot 50.3$	Area of mild compression steel [mm^2]
$d' := 30$	Depth to the mild compression steel centroid [mm]
$As2' := 0$	Second area of mild compression steel [mm^2]
$d2' := 50$	Depth to the second mild compression steel centroid [mm]
$Ap := 0$	Area of prestressing steel [mm^2]
$dp := 378$	Depth to the prestressing steel centroid [mm]
$fpe := 0$	Effective stress in the steel due to prestress [MPa]
$Bond := 1$	Type of tendon installation (Enter "1" for bonded, "0" for unbonded)
$dt := d$	Distance from extreme compression fiber to centroid of extreme layer of longitudinal tension steel, (Chapters 9, 10, Appendix C ACI 318-05)

Load and Span Information

$Mu := 24.2$	Factored moment to be resisted by the strengthened element [kN-m]
$M_{DL} := 0.3 \cdot Mu$	Unfactored dead load moment to be resisted by the strengthened element [kN-m]
$M_{LL} := 0.3 \cdot Mu$	Unfactored live load moment to be resisted by the strengthened element [kN-m]
$Mip := M_{DL}$	Moment in place at the time of FRP installation [kN-m]

$ln := 0$	Clear span [m]
$lr := 1.0$	Ratio of loaded spans to total spans (e.g., 0.50 for alternate bay loading) This variable is used only if unbonded tendons are present

Material Property Specifications

$f'c := 36$	Nominal compressive strength of the concrete [MPa]
$Conc := 1$	Type of Concrete 1 -- Normal Weight Concrete 2 -- All-Lightweight Concrete 3 -- Sand-Lightweight Concrete
$\gamma_c = 1$	Strength reduction factor based on concrete type
$fy := 460$	Yield strength of the mild steel [MPa]
$fpu := 1720$	Ultimate strength of the prestressing steel [MPa]
$fpy := 1560$	Yield strength of the prestressing steel [MPa]
$Ep := 195000$	Modulus of elasticity of the prestressing steel [MPa]

Results of the Flexural Strengthening Analysis

Design Ultimate Moment Capacity

$\phi Mn = 24.2$ $\quad Mu = 24.2$ $\quad$ Design moment capacity vs moment demand [kN-m]

Strain Distribution at Ultimate

$cu = 28$	Depth to the neutral axis [mm]
$\varepsilon cu = 0.003$	Maximum strain in the concrete
$\varepsilon s'(\varepsilon cu, cu) = -0.0002$	Strain in the mild compression steel
$\varepsilon s(\varepsilon cu, cu) = 0.0257$	Strain in the mild tension steel
$\varepsilon ps(\varepsilon cu, cu) = 0$	Strain in the prestressing steel

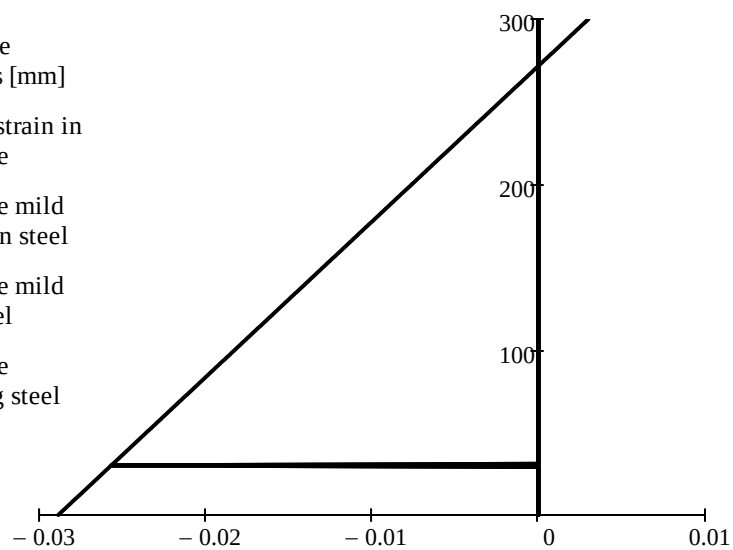

Check of Design Limits

$fcs = 11.68$	$Fcs = 16$	Concrete stress at service vs service stress limit [MPa] (Limit applicable to prestressed members only)
$fss = 258$	$Fss = 368$	Mild tension steel stress at service vs service stress limit [MPa]
$fpss = 0$	$Fps = 1273$	Prestressing steel stress at service vs service stress limit [MPa]

Detailed Calculation of the Design Moment Capacity

Computation of Gross Section Properties

- Effective width of concrete in compression [mm]

  $be := \text{if}(bft = 0, bw, bft)$

  $be = 150$

- Cross sectional area [mm²]

  $Ac := bw \cdot h + (bft - bw) \cdot tft + (bfb - bw) \cdot tfb$

  $Ac = 45000$

- Distance from the top fiber to the centroid [mm]

  $$ct := \frac{0.5 \cdot bw \cdot h^2 + 0.5 \cdot (bft - bw) \cdot tft^2 + (bfb - bw) \cdot tfb \cdot (h - 0.5 \cdot tfb)}{Ac}$$

  $ct = 150$

- Distance from the bottom fiber to the centroid [mm]

  $cb := h - ct$

  $cb = 150$

- Gross moment of inertia [mm⁴]

  $$Ig := bw \cdot h \cdot \left[\frac{h^2}{12} + \left(\frac{h}{2} - ct\right)^2\right] + (bft - bw) \cdot tft \cdot \left[\frac{tft^2}{12} + \left(ct - \frac{tft}{2}\right)^2\right] + (bfb - bw) \cdot tfb \cdot \left[\frac{tfb^2}{12} + \left(cb - \frac{tfb}{2}\right)^2\right]$$

  $Ig = 3.375 \times 10^8$

- Radius of gyration [mm]

  $$r := \sqrt{\frac{Ig}{Ac}}$$

  $r = 87$

Computation of Material Characteristics

- Modulus of elasticity for concrete [MPa]

  $Ec := 0.043 \cdot wc^{1.5} \cdot \sqrt{f'c}$

  $Ec = 3.039 \times 10^4$

- Concrete strain corresponding to f'c [mm/mm]

  $$\varepsilon'c := \frac{1.71 \cdot f'c}{Ec}$$

  $\varepsilon'c = 2.03 \times 10^{-3}$

- Yield strain for the mild reinforcement [mm/mm]

  $$\varepsilon sy := \frac{fy}{Es}$$

  $\varepsilon sy = 2.3 \times 10^{-3}$

Preliminary computations for prestressing steel properties

- Prestressing force [N]

  $Pe := Ap \cdot fpe$

  $Pe = 0$

- Eccentricity of prestressing force [mm]

  $e := dp - ct$

  $e = -151$

- Strain in the tendon at decompression [mm/mm]

  $$\varepsilon p1 := \frac{Pe}{Ap \cdot Ep} + \frac{Pe}{Ac \cdot Ec} \cdot \left(1 + \frac{e^2}{r^2}\right)$$

  $\varepsilon p1 = 0$

- Bond reduction coefficient applied to unbonded tendons

  $$\Omega b := \text{if}\left(Bond = 0, \frac{3.0}{\frac{ln}{dp}} \cdot lr, 1.0\right)$$

  $\Omega b = 1$

Moment capacity calculation based on the failure mode, strain compatibility, and equilibrium

- Compute the moment at service level [kN-m]

  $Ms := M_{DL} + M_{LL}$

  $Ms = 14.52$

- Find the depth to the neutral axis by trial and error [mm]

  $c = 28.26$

- Compute the strain in the concrete if failure is controlled by concrete crushing (Failure Mode 1) [mm/mm]

  $\varepsilon c1 := 0.003$

- Compute the strain in the concrete if failure is controlled by tendon rupture (Failure Mode 2) [mm/mm]

  $$\varepsilon c2 := \begin{cases} 0.003 & \text{if } Ap = 0 \\ \text{otherwise} & \\ \quad \begin{cases} (0.03 - \varepsilon p1) \cdot \dfrac{c}{dp - c} & \text{if } Bond = 1 \\ \dfrac{1}{\Omega b} \cdot \left(\dfrac{0.94 \cdot fpy}{Ep} - \varepsilon p1\right) \cdot \dfrac{c}{dp - c} & \text{if } Bond = 0 \end{cases} \end{cases}$$

  $\varepsilon c2 = 0.003$

- Compute the strain in the concrete based on which mode of failure governs [mm/mm]

  $\varepsilon c := \min(\varepsilon c1, \varepsilon c2)$

  $\varepsilon c = 0.003$

- Compute the strain in the mild compression steel at ultimate [mm/mm]

$$\varepsilon s' := \begin{cases} 0 & \text{if } As' = 0 \\ \varepsilon c \cdot \dfrac{c - d'}{c} & \text{otherwise} \end{cases}$$

$\varepsilon s' = -1.847 \times 10^{-4}$

$$\varepsilon s2' := \begin{cases} 0 & \text{if } As2' = 0 \\ \varepsilon c \cdot \dfrac{c - d2'}{c} & \text{otherwise} \end{cases}$$

$\varepsilon s2' = 0$

- Compute the strain in the mild tension steel at ultimate [mm/mm]

$$\varepsilon s := \begin{cases} 0 & \text{if } As = 0 \\ \varepsilon c \cdot \dfrac{d - c}{c} & \text{otherwise} \end{cases}$$

$\varepsilon s = 0.026$

$$\varepsilon s2 := \begin{cases} 0 & \text{if } As2 = 0 \\ \varepsilon c \cdot \dfrac{d2 - c}{c} & \text{otherwise} \end{cases}$$

$\varepsilon s2 = 0$

- Compute the strain in the prestressing steel at ultimate [mm/mm]

$$\varepsilon ps := \begin{cases} 0 & \text{if } Ap = 0 \\ \varepsilon p1 + \Omega b \cdot \varepsilon c \cdot \dfrac{dp - c}{c} & \text{otherwise} \end{cases}$$

$\varepsilon ps = 0$

- Compute the stress in the mild compression steel at ultimate for elastic/perfectly plastic behavior [MPa]

$$fs' := \begin{cases} fy & \text{if } \varepsilon s' > \varepsilon sy \\ -fy & \text{if } \varepsilon s' < -\varepsilon sy \\ Es \cdot \varepsilon s' & \text{otherwise} \end{cases}$$

$fs' = -37$

$$fs2' := \begin{cases} fy & \text{if } \varepsilon s2' > \varepsilon sy \\ -fy & \text{if } \varepsilon s2' < -\varepsilon sy \\ Es \cdot \varepsilon s2' & \text{otherwise} \end{cases}$$

$fs2' = 0$

- Compute the stress in the mild tension steel at ultimate for elastic/perfectly plastic behavior [MPa]

$$fs := \begin{cases} fy & \text{if } \varepsilon s > \varepsilon sy \\ -fy & \text{if } \varepsilon s < -\varepsilon sy \\ Es \cdot \varepsilon s & \text{otherwise} \end{cases}$$

$fs = 460$

$$fs2 := \begin{cases} fy & \text{if } \varepsilon s2 > \varepsilon sy \\ -fy & \text{if } \varepsilon s2 < -\varepsilon sy \\ Es \cdot \varepsilon s2 & \text{otherwise} \end{cases}$$

$fs2 = 0$

- Compute the stress in the prestressing steel at ultimate per PCI Design Aid 11.2.5 [MPa]

$$fps := \begin{cases} \text{if } fpu = 1720 \\ \quad \begin{cases} \varepsilon ps \cdot Ep & \text{if } \varepsilon ps \le 0.0076 \\ \left(1720 - \dfrac{0.276}{\varepsilon ps - 0.0064}\right) & \text{if } \varepsilon ps > 0.0076 \end{cases} \\ \text{if } fpu = 1860 \\ \quad \begin{cases} \varepsilon ps \cdot Ep & \text{if } \varepsilon ps \le 0.0086 \\ \left(1860 - \dfrac{0.276}{\varepsilon ps - 0.007}\right) & \text{if } \varepsilon ps > 0.0086 \end{cases} \end{cases}$$

$fps = 0$

- Todeschini's equation defining the nonlinear compressive stress distribution in the concrete:

$$fc(y) := \frac{1.8 \cdot f'c \cdot \left(\dfrac{\varepsilon c \cdot y}{\varepsilon' c \cdot c}\right)}{1 + \left(\dfrac{\varepsilon c \cdot y}{\varepsilon' c \cdot c}\right)^2}$$

- Find the resultant compressive force from the compressive stress distribution in the concrete [N]

$$Cc := \int_0^c fc(y) \cdot be \, dy - \text{if}(bft = 0, 0, 1) \cdot \text{if}(c < tft, 0, 1) \cdot \int_0^{c-tft} fc(y) \cdot (be - bw) \, dy$$

- Check internal force equilibrium by summing the internal force resultants. Revise "c" if the sum does not equal zero.

$$\Sigma F := Cc + As' \cdot fs' + As2' \cdot fs2' - As \cdot fs - As2 \cdot fs2 - Ap \cdot fps$$

$\Sigma F = 0$ O.K.

- Locate the centroid of the compressive stress distribution in the concrete [mm]

$$\beta c := 2 \cdot \left[c - \frac{\displaystyle\int_0^c fc(y) \cdot be \cdot y \, dy - \text{if}(bft = 0, 0, 1) \cdot \text{if}(c < tft, 0, 1) \cdot \int_0^{c-tft} fc(y) \cdot (be - bw) \cdot y \, dy}{Cc} \right]$$

$\beta c = 23.38$

- Compute the strength reduction factor based on ductility per ACI 318-05 Section B.9.3.2.

$$\phi := \begin{cases} 0.9 & \text{if } \frac{c}{dt} \le 0.375 \\ 0.65 + 0.25\cdot\left(\frac{dt}{c} - \frac{5}{3}\right) & \text{if } \frac{c}{dt} < 0.6 \wedge \frac{c}{dt} > 0.375 \\ 0.65 & \text{if } \frac{c}{dt} \ge 0.6 \end{cases}$$

$\phi = 0.9$

- Compute the contribution to the design moment capacity of the mild and prestressing steel reinforcement [kN-m]

$$\phi Mn := \phi\cdot\frac{1}{10^6}\cdot\left[\begin{array}{l} As'\cdot fs'\cdot\left(\frac{\beta c}{2} - d'\right) + As2'\cdot fs2'\cdot\left(\frac{\beta c}{2} - d2'\right) + As\cdot fs\cdot\left(d - \frac{\beta c}{2}\right) + As2\cdot fs2\cdot\left(d2 - \frac{\beta c}{2}\right) \ldots \\ + Ap\cdot fps\cdot\left(dp - \frac{\beta c}{2}\right) \end{array}\right]$$

$\phi Mn = 24.23$

APPENDIX D – CONTROL CALCULATIONS

Flexural Strengthening Design ACI 440.2R-08 - CFRP Sheets & Rods

Project: Masters Thesis

Condition: Strengthened Beam wih 1 ply of CFRP

Levels: ----

Designed by: KH

Date: 17th April 2017

STRUCTURAL TECHNOLOGIES
7455-T New Ridge Road
Hanover, MD 21076-3143 USA
Tel: 410-850-7000 Fax: 410-850-4111
www.structural.net

Required Information about the Existing Structure

Section Dimensions

$h := 300$ Total section height [mm]

$bw := 150$ Width of web [mm]

$bft := 0$ Width of top flange (zero for rectangular or inverted tee sections) [mm]

$tft := 0$ Thickness of top flange (zero for rectangular or inverted tee sections) [mm]

$bfb := 0$ Width of bottom flange (zero for rectangular or tee sections) [mm]

$tfb := 0$ Thickness of bottom flange (zero for rectangular or tee sections) [mm]

Reinforcement Layout

$As := 2 \cdot 113$ Area of mild tension steel [mm^2]

$d := h - 30$ Depth to the mild tension steel centroid [mm]

$As2 := 0 \cdot 0$ Second Area of mild tension steel [mm^2]

$d2 := d$ Depth to the second mild tension steel centroid [mm]

$As' := 2 \cdot 50.3$ Area of mild compression steel [mm^2]

$d' := 30$ Depth to the mild compression steel centroid [mm]

$As2' := 0$ Second area of mild compression steel [mm^2]

$d2' := 50$ Depth to the second mild compression steel centroid [mm]

Load and Span Information

$\phi Mn_{orig} := 24.2$ Flexural strength of the unstrengthened element [kN-m]

$Mu := 44.6$ Factored moment to be resisted by the strengthened element [kN-m]

$M_{DL} := 0.3 \cdot Mu$ Dead load moment to be resisted by the strengthened element [kN-m]

$M_{LL} := 0.3 \cdot Mu$ Live load moment to be resisted by the strengthened element [kN-m]

$Mip := M_{DL}$ Moment in place at the time of FRP installation [kN-m]

$ln := 0$ Clear span [m] This variable is used only if unbonded tendons are present

$lr := 1.0$ Ratio of loaded spans to total spans (e.g., 0.50 for alternate bay loading)
This variable is used only if unbonded tendons are present

Material Property Specifications

$fcu := 45$ Nominal cubic compressive strength of the concrete [MPa]

$f'c := 36$ Nominal cylindrical compressive strength of the concrete [MPa]

$fy := 460$ Yield strength of the mild steel [MPa]

Required FRP Design Information

FRP Material Selection

$Fiber := 3$ FRP Reinforcement

1 -- V-Wrap C100 High Strength Carbon Fiber (300g/m^2)
2 -- V-Wrap C180 High Strength Carbon Fiber (580g/m^2)
3 -- V-Wrap C200-H High Strength Carbon Fiber (750g/m^2)

$ffu^* = 1100$ Ultimate tensile strength of the FRP [MPa]

$\varepsilon fu^* = 0.013$ Ultimate rupture strain of the FRP [mm/mm]

$Ef = 72080$ Tensile modulus of elasticity of the FRP [MPa]

$tf = 1.02$ Nominal design thickness of one ply of the FRP [mm/ply]

Additional Design Parameters

$Ccr := 0.55$ Creep rupture stress limit (Use 0.55 for Carbon, 0.30 for Aramid, and 0.20 for E-Glass)

$Exposure := 1$ Exposure Condition

1 -- Interior Exposure
2 -- Exterior Exposure
3 -- Aggressive Exposure

$Ce = 0.95$ Enviromental reduction factor for FRP reinforcement

Layout of the FRP Sheets Reinforcement

$wf := 150$ Width of the fiber strip [mm]

$n := 1$ Number of fiber plies

NSM FRP Bars Reinforcement

$Bar_Size := 12$ Select available bar sizes #10 (US-#3) or #12 (US-#4)

$ffu_bar = 1860$ Ultimate tensile strength of the FRP bar [MPa]

$\varepsilon fu_bar = 0.015$ Ultimate rupture strain of the FRP bar [mm/mm]

$Ef_bar = 127500$ Tensile modulus of elasticity of the FRP bar [MPa]

$Af_bar = 122.58$ Nominal cross-sectional area of FRP bar [mm^2]

$n_bar := 0$ Number of FRP bars

$d_bar = 287$ Depth to the FRP bar centroid [mm]

Results of the Flexural Strengthening Analysis

Design Ultimate Moment Capacity

$\phi Mn = 44.6$ $\quad Mu = 44.6$ $\quad$ Design moment capacity vs moment demand [kN-m]

Strain Distribution at Ultimate

$cu = 53.56$	Depth to the neutral axis [mm]
$\varepsilon cu = 0.0023$	Maximum strain in the concrete
$\varepsilon s'(\varepsilon cu, cu) = 0.001$	Strain in the mild compression steel
$\varepsilon s(\varepsilon cu, cu) = 0.0092$	Strain in the mild tension steel
$\varepsilon ps(\varepsilon cu, cu) = 0$	Strain in the prestressing steel
$\varepsilon f_bar(\varepsilon cu, cu) = 0$	Strain in NSM bars
$\varepsilon f(\varepsilon cu, cu) = 0.0091$	Strain in the FRP sheets

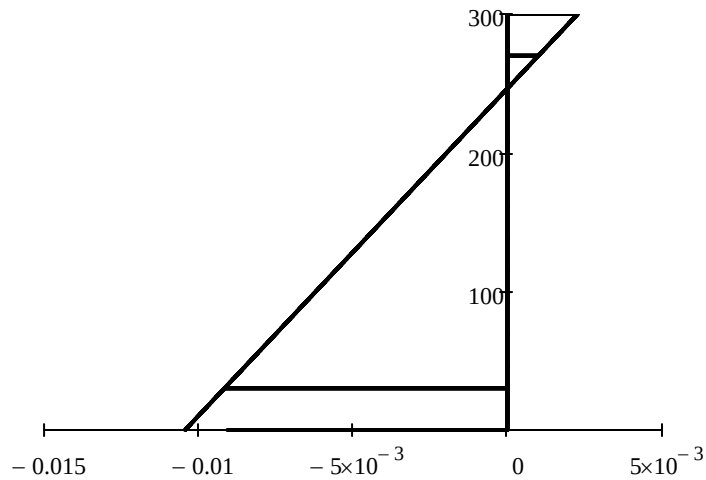

Check of Design Limits

$fcs = 12$	$Fcs = 18$	Concrete stress at service vs service stress limit (0.4 fcu) [MPa] (Limit applicable to prestressed members only)
$fss = 422$	$Fss = 368$	Mild tension steel stress at service vs service stress limit [MPa]
$fpss = 0$	$Fps = 1273$	Prestressing steel stress at service vs service stress limit [MPa]
$ffs = 67$	$Ffs = 575$	FRP sheets service stress vs creep rupture stress limit [MPa]
$ffs_bar = 0$	$Ffs_bar = 972$	NSM bars service stress vs creep rupture stress limit [MPa]
$\phi Mn_{orig} = 24.2$	$\phi Mn_{min} = 25$	Existing strength vs minimum strength limit [kN-m]

Detailed Calculation of the Design Moment Capacity

Computation of Gross Section Properties

- Effective width of concrete in compression [mm]

  $be := if(bft = 0, bw, bft)$

  $be = 150$

- Cross sectional area [mm²]

  $Ac := bw \cdot h + (bft - bw) \cdot tft + (bfb - bw) \cdot tfb$

  $Ac = 45000$

- Distance from the top fiber to the centroid [mm]

$$ct := \frac{0.5 \cdot bw \cdot h^2 + 0.5 \cdot (bft - bw) \cdot tft^2 + (bfb - bw) \cdot tfb \cdot (h - 0.5 \cdot tfb)}{Ac}$$

$ct = 150$

- Distance from the bottom fiber to the centroid [mm]

$cb := h - ct$

$cb = 150$

- Gross moment of inertia [mm^4]

$$Ig := bw \cdot h \cdot \left[\frac{h^2}{12} + \left(\frac{h}{2} - ct\right)^2\right] + (bft - bw) \cdot tft \cdot \left[\frac{tft^2}{12} + \left(ct - \frac{tft}{2}\right)^2\right] + (bfb - bw) \cdot tfb \cdot \left[\frac{tfb^2}{12} + \left(cb - \frac{tfb}{2}\right)^2\right]$$

$Ig = 3.375 \times 10^8$

- Radius of gyration [mm]

$$r := \sqrt{\frac{Ig}{Ac}}$$

$r = 87$

Computation of Material Characteristics

- Modulus of elasticity for concrete [MPa]

$Ec := 4731 \cdot \sqrt{f'c}$

$Ec = 2.839 \times 10^4$

- Concrete strain corresponding to f'c [mm/mm]

$$\varepsilon'c := \frac{1.71 \cdot f'c}{Ec}$$

$\varepsilon'c = 2.169 \times 10^{-3}$

- Yield strain for the mild reinforcement [mm/mm]

$$\varepsilon sy := \frac{fy}{Es}$$

$\varepsilon sy = 2.3 \times 10^{-3}$

Preliminary computations for properties of FRP sheets

- Design ultimate tensile strength [MPa]

$ffu := Ce \cdot ffu^*$

$ffu = 1045$

- Design rupture strain [mm/mm]

$\varepsilon fu := Ce \cdot \varepsilon f\check{u}$

$\varepsilon fu = 0.012$

- FRP sheets design strain for flexure [mm/mm]

$$\varepsilon fd := \min\left(0.41\cdot\sqrt{\frac{f'c}{n\cdot Ef\cdot tf}},\ 0.9\cdot\varepsilon fu\right)$$

$$\varepsilon fd = 9.073\times 10^{-3}$$

Preliminary computations for properties of FRP bars:

- Design ultimate tensile strength [MPa]

$$ffu_bar := Ce\cdot ffu^{*}_bar$$

$$ffu_bar = 1767$$

- Design rupture strain [mm/mm]

$$\varepsilon fu_bar := Ce\cdot \varepsilon fu^{*}_bar$$

$$\varepsilon fu_bar = 0.014$$

- FRP bars design strain for flexure [mm/mm]

$$\kappa m_bar := 0.7$$

$$\varepsilon fd_bar := \kappa m_bar\cdot \varepsilon fu_bar$$

$$\varepsilon fd_bar = 9.975\times 10^{-3}$$

Moment capacity calculation based on the failure mode, strain compatibility, and equilibrium

- Compute the moment at service level [kN-m]

$$Ms := M_{DL} + M_{LL}$$

$$Ms = 26.76$$

- Find the depth to the neutral axis by trial and error [mm]

$$c = 53.561$$

- Compute the strain in the concrete if failure is controlled by concrete crushing (Failure Mode 1) [mm/mm]

$$\varepsilon c1 := 0.003$$

- Compute the strain in the concrete if failure is controlled by tendon rupture (Failure Mode 2) [mm/mm]

$$\varepsilon c2 := \begin{cases} 0.003 & \text{if } Ap = 0 \\ \text{otherwise} & \\ \quad \begin{cases} (0.03-\varepsilon p1)\cdot\dfrac{c}{dp-c} & \text{if } Bond = 1 \\ \dfrac{1}{\Omega b}\cdot\left(\dfrac{0.94\cdot fpy}{Ep}-\varepsilon p1\right)\cdot\dfrac{c}{dp-c} & \text{if } Bond = 0 \end{cases} & \end{cases}$$

$$\varepsilon c2 = 0.003$$

- Compute the strain in the concrete if failure is controlled by FRP failure (Failure Mode 3) [mm/mm]

$$\varepsilon c3 := \begin{cases} 0.003 & \text{if } Af_t = 0 \wedge Af_bar_t = 0 \\ \left[(\varepsilon fd + \varepsilon bi)\cdot\dfrac{c}{h-c}\right] & \text{if } Af_bar_t = 0 \wedge Af_t \neq 0 \\ \left[(\varepsilon fd_bar + \varepsilon bi)\cdot\dfrac{c}{d_bar-c}\right] & \text{if } Af_t = 0 \wedge Af_bar_t \neq 0 \\ \min\left[\left[(\varepsilon fd + \varepsilon bi)\cdot\dfrac{c}{h-c}\right],\left[(\varepsilon fd_bar + \varepsilon bi_bar)\cdot\dfrac{c}{d_bar-c}\right]\right] & \text{otherwise} \end{cases}$$

$\varepsilon c3 = 0.0023$

- Compute the strain in the concrete based on which mode of failure governs [mm/mm]

$\varepsilon c := \min((\varepsilon c1 \quad \varepsilon c2 \quad \varepsilon c3))$

$\varepsilon c = 0.0023$

- Compute the strain in the mild compression steel at ultimate [mm/mm]

$$\varepsilon s' := \begin{cases} 0 & \text{if } As' = 0 \\ \varepsilon c\cdot\dfrac{c-d'}{c} & \text{otherwise} \end{cases}$$

$\varepsilon s' = 9.978 \times 10^{-4}$

$$\varepsilon s2' := \begin{cases} 0 & \text{if } As2' = 0 \\ \varepsilon c\cdot\dfrac{c-d2'}{c} & \text{otherwise} \end{cases}$$

$\varepsilon s2' = 0$

- Compute the strain in the mild tension steel at ultimate [mm/mm]

$$\varepsilon s := \begin{cases} 0 & \text{if } As = 0 \\ \varepsilon c\cdot\dfrac{d-c}{c} & \text{otherwise} \end{cases}$$

$\varepsilon s = 9.167 \times 10^{-3}$

$$\varepsilon s2 := \begin{cases} 0 & \text{if } As2 = 0 \\ \varepsilon c\cdot\dfrac{d2-c}{c} & \text{otherwise} \end{cases}$$

$\varepsilon s2 = 0$

- Compute the strain in the FRP sheets at ultimate [in/in or mm/mm]

$$\varepsilon f := \begin{cases} 0 & \text{if } Af_t = 0 \\ \varepsilon c\cdot\dfrac{h-c}{c} - \varepsilon bi & \text{otherwise} \end{cases}$$

$\varepsilon f = 9.073 \times 10^{-3}$

<u>Note:</u> Based on M_{ip}, the initial strain in the substrate was computed to be:

$\varepsilon bi = 0.001$

- Compute the strain in the NSM bars at ultimate [mm/mm]

$$\varepsilon f_bar := \begin{cases} 0 & \text{if } Af_bar_t = 0 \\ \varepsilon c \cdot \dfrac{d_bar - c}{c} - \varepsilon bi_bar & \text{otherwise} \end{cases}$$

$\varepsilon f_bar = 0$

Note: Based on M_{ip}, the initial strain in the substrate was computed to be:

$\varepsilon bi_bar = -0$

- Compute the stress in the mild compression steel at ultimate for elastic/perfectly plastic behavior [MPa]

$$fs' := \begin{cases} fy & \text{if } \varepsilon s' > \varepsilon sy \\ -fy & \text{if } \varepsilon s' < -\varepsilon sy \\ Es \cdot \varepsilon s' & \text{otherwise} \end{cases}$$

$fs' = 200$

$$fs2' := \begin{cases} fy & \text{if } \varepsilon s2' > \varepsilon sy \\ -fy & \text{if } \varepsilon s2' < -\varepsilon sy \\ Es \cdot \varepsilon s2' & \text{otherwise} \end{cases}$$

$fs2' = 0$

- Compute the stress in the mild tension steel at ultimate for elastic/perfectly plastic behavior [MPa]

$$fs := \begin{cases} fy & \text{if } \varepsilon s > \varepsilon sy \\ -fy & \text{if } \varepsilon s < -\varepsilon sy \\ Es \cdot \varepsilon s & \text{otherwise} \end{cases}$$

$fs = 460$

$$fs2 := \begin{cases} fy & \text{if } \varepsilon s2 > \varepsilon sy \\ -fy & \text{if } \varepsilon s2 < -\varepsilon sy \\ Es \cdot \varepsilon s2 & \text{otherwise} \end{cases}$$

$fs2 = 0$

- Compute the stress in the FRP sheets at ultimate by Hooke's Law [MPa]

$ff := Ef \cdot \varepsilon f$

$ff = 654$

- Compute the stress in the NSM bars at ultimate by Hooke's Law [MPa]

$ff_bar := Ef_bar \cdot \varepsilon f_bar$

$ff_bar = 0$

- Todeschini's equation defining the nonlinear compressive stress distribution in the concrete:

$$fc(y) := \frac{1.8 \cdot f'c \cdot \left(\dfrac{\varepsilon c \cdot y}{\varepsilon' c \cdot c}\right)}{1 + \left(\dfrac{\varepsilon c \cdot y}{\varepsilon' c \cdot c}\right)^2}$$

- Find the resultant compressive force from the compressive stress distribution in the concrete [N]

$$Cc := \int_0^{c} fc(y)\cdot be\ dy - if(bft = 0, 0, 1)\cdot if(c < tft, 0, 1)\cdot \int_0^{c-tft} fc(y)\cdot(be - bw)\ dy \qquad Cc = 1.839 \times 10^5$$

- Check internal force equilibrium by summing the internal force resultants. Revise "c" if the sum does not equal zero.

$$\Sigma F := Cc + As'\cdot fs' + As2'\cdot fs2' - As\cdot fs - As2\cdot fs2 - Ap\cdot fps - Af_t\cdot ff - Af_bar_t\cdot ff_bar$$

$\Sigma F = -0$ O.K.

- Locate the centroid of the compressive stress distribution in the concrete [mm]

$$\beta c := 2\cdot\left[c - \frac{\int_0^{c} fc(y)\cdot be\cdot y\ dy - if(bft = 0, 0, 1)\cdot if(c < tft, 0, 1)\cdot \int_0^{c-tft} fc(y)\cdot(be - bw)\cdot y\ dy}{Cc}\right]$$

$\beta c = 41.14$

- Additional reduction factor applied to the FRP contribution

$\psi f := 0.85$

- Compute the strength reduction factor based on ductility per ACI 318-05 Section B.9.3.2.

$$\phi := \begin{cases} 0.9 & \text{if } \frac{c}{dt} \le 0.375 \\ 0.65 + 0.25\cdot\left(\frac{dt}{c} - \frac{5}{3}\right) & \text{if } \frac{c}{dt} < 0.6 \wedge \frac{c}{dt} > 0.375 \\ 0.65 & \text{if } \frac{c}{dt} \ge 0.6 \end{cases}$$

$\phi = 0.9$

- Compute the contribution to the design moment capacity of the mild and prestressing steel reinforcement [kN-m]

$$\phi Mn1 := \phi\cdot\frac{1}{10^6}\cdot\left[As'\cdot fs'\cdot\left(\frac{\beta c}{2} - d'\right) + As2'\cdot fs2'\cdot\left(\frac{\beta c}{2} - d2'\right) + As\cdot fs\cdot\left(d - \frac{\beta c}{2}\right) + As2\cdot fs2\cdot\left(d2 - \frac{\beta c}{2}\right) \ldots + Ap\cdot fps\cdot\left(dp - \frac{\beta c}{2}\right)\right]$$

$\phi Mn1 = 23.17$

- Compute the contribution to the design moment capacity of FRP sheets [kN-m]

$$\phi Mn2 := \phi\cdot\frac{1}{10^6}\cdot\left[\psi f\cdot Af_t\cdot ff\cdot\left(h - \frac{\beta c}{2}\right)\right]$$

$\phi Mn2 = 21.388$

- Compute the contribution to the design moment capacity of FRP bars [kN-m]

$$\phi Mn3 := \phi\cdot\frac{1}{10^6}\cdot\left[\psi f\cdot Af_bar_t\cdot ff_bar\cdot\left(d_bar - \frac{\beta c}{2}\right)\right]$$

$\phi Mn3 = 0$

- Compute the design moment capacity [kN-m]

$\phi Mn := \phi Mn1 + \phi Mn2 + \phi Mn3$

$\phi Mn = 44.56$

- Compute the limit for minimum moment capacity of the unstrengthened member [kN-m]

$\phi Mn_{min} := \left(1.1 \cdot M_{DL} + 0.75 \cdot M_{LL}\right)$

$\phi Mn_{min} = 24.75$

Vita

Kareem Helal was born in 1991, in Abu Dhabi, United Arab Emirates. He received his primary education in Sharjah and secondary education in Dubai, UAE. He received his B.Sc. degree in Civil Engineering from the American University of Sharjah in June 2013. For the first 6 months, he worked as a Structural Engineer at Bin Dalmouk Consultants. In September 2014, Kareem joined SPME Middle East General Contracting, a Structural group company, and has been working as a Project Engineer since then.

In September 2013, he joined the Civil Engineering master's program in the American University of Sharjah and worked as a graduate teaching assistant for 3 semesters. During his undergraduate study, he published a Journal Paper in the International Journal of Concrete Structures and Materials. During his Masters study, he has presented research works in Singapore at the ACE2015 conference. His research interests are in mechanical and durability behaviour of concrete and structural strengthening.